Published by Institute of Physics Publishing for SISSA
Received: *February 4, 2008*
Accepted: *March 11, 2008*
Published: *March 25, 2008*

JHEP03(2008)058

# Anomalies and O-plane charges in orientifolded brane tilings

**Yosuke Imamura, Keisuke Kimura and Masahito Yamazaki**

*Department of Physics, University of Tokyo,*
*Tokyo 113-0033, Japan*
*E-mail:* imamura@hep-th.phys.s.u-tokyo.ac.jp,
kimura@hep-th.phys.s.u-tokyo.ac.jp, yamazaki@hep-th.phys.s.u-tokyo.ac.jp

Abstract: We investigate orientifold of brane tilings. We clarify how the cancellations of gauge anomaly and Witten's anomaly are guaranteed by the conservation of the D5-brane charge. We also discuss the relation between brane tilings and the dual Calabi-Yau cones realized as the moduli spaces of gauge theories. Two types of flavor D5-branes in brane tilings and corresponding superpotentials of fundamental quark fields are proposed, and it is shown that the massless loci of these quarks in the moduli space correctly reproduce the worldvolume of flavor D7-branes in the Calabi-Yau cone dual to the fivebrane system.

Keywords: Anomalies in Field and String Theories, D-branes, Supersymmetric gauge theory.

## Contents



JHEP03(2008)058

## 1. Introduction

Brane tilings [1 – 3] are two-dimensional diagrams drawn on tori which are used to represent the structure of a large class of quiver gauge theories. They can be used to describe arbitrary $\mathcal{N} = 1$ superconformal field theories realized on D3-branes in toric Calabi-Yau cones. They are dual graphs of corresponding quiver diagrams, and vertices and edges in a graph represent SU($N$) factors in the gauge group and chiral multiplets belonging to bi-fundamental representations. The graphs are bipartite. Namely, vertices are colored black and white, and any pair of vertices connected by an edge have different colors. The orientation of edges are determined according to the colors of vertices at the endpoints. We take it from black to white. Because SU($N$) factors correspond to faces, it is natural to represent a bi-fundamental field $\Phi^a{}_b$ as an arrow connecting two adjacent faces for two

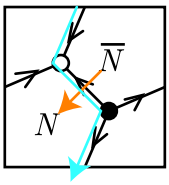


**Figure 1:** The bipartite graph of $\mathbb{C}^3$ is shown. This diagram has two vertices of opposite colors, three edges from black to white, and one hexagonal face. Among three arrows representing three adjoint fields and three zig-zag paths representing the boundary of semi-infinite cylinders of NS5-branes, one for each is shown.

| | 0 | 1 | 2 | 3 | 4 | 5 | 6 | 7 | 8 | 9 |
|---|---|---|---|---|---|---|---|---|---|---|
| D5 | ○ | ○ | ○ | ○ | | ○ | | ○ | | |
| NS5 | ○ | ○ | ○ | ○ | | $\Sigma$ | | | | |

**Table 1:** The structure of fivebrane systems represented by brane tilings.

SU($N$) factors coupling to $\Phi^a{}_b$. The orientation of arrows, which specifies one of $(N, \overline{N})$ or $(\overline{N}, N)$, is also determined with the colors of vertices. We take the convention that if the orientation of an edge is South to North the orientation of the arrow intersecting with the edge is East to West. The head and tail of an arrow correspond to the upper color index for the fundamental representation and the lower color index for the anti-fundamental representation, respectively (figure 1).

The important feature of brane tilings is that they are directly related to the topological structure of fivebrane systems realizing the gauge theories, as is clarified in [4]. We can regard the torus on which a bipartite graph is drawn as a stack of D5-branes, and edges in the bipartite graph as NS5-branes intersecting with the D5-branes. We can reconstruct the worldvolume of the NS5-brane by attaching semi-infinite cylinders to the torus along zig-zag paths in the diagram. A zig-zag path is a path made of edges in a bipartite graph defined so that when we go along the path we choose the leftmost edge at white vertices and the rightmost edge at black vertices. We can regard a bipartite graph as the superposition of zig-zag paths. Because every edge is included in two zig-zag paths, each edge can be regarded as a part of the intersection of D5-branes and NS5-branes.

We label four dimensions in which the gauge theory lives by 0123, and the two cycles in the torus by 5 and 7. The orientation of branes in the system is shown in table 1. $\Sigma$ in the table is a two-dimensional non-compact surface in 4567 space. All branes are in the subspace $x^8 = x^9 = 0$, and the system possesses the rotational symmetry on 89-plane. This is an R-symmetry in the gauge theory, which is not necessarily the R-symmetry in the superconformal group unless it is appropriately mixed with the gauge symmetries on the fivebrane system. In the weak string coupling limit the tension of NS5-branes becomes infinitely larger than that of D5-branes, and the worldvolume of the NS5-brane becomes a



JHEP03(2008)058

| | 0 | 1 | 2 | 3 | 4 | 5 | 6 | 7 | 8 | 9 |
|---|---|---|---|---|---|---|---|---|---|---|
| D5 | ○ | ○ | ○ | ○ | | ○ | | ○ | | |
| NS5 | ○ | ○ | ○ | ○ | | Σ | | | | |
| O5 | ○ | ○ | ○ | ○ | ○ | | ○ | | | |
| O7 | ○ | ○ | ○ | ○ | ○ | | | ○ | ○ | ○ |

**Table 2:** The structure of fivebrane systems with orientifolds. As shown in this table, both O5-planes and O7-planes preserve $\mathcal{N} = 1$ supersymmetry. In this paper we only consider the case of O5-planes.

smooth holomorphic surface in the 4567 space. It is given by

$$P(e^{x^4+ix^5}, e^{x^6+ix^7}) = 0, \tag{1.1}$$

where $P(u, v)$ is the Newton polynomial associated with the toric diagram of the toric Calabi-Yau cone. The NS5-brane worldvolume has branches going to infinity on the 46-plane. Each branch of NS5-brane is topologically semi-infinite cylinder, which is attached on the D5-branes along a zig-zag path. The asymptotic structure of NS5-brane projected on the 46-plane gives the web-diagram of the Calabi-Yau, while the brane tiling can be regarded as the projection of NS5-branes into the 57-plane. This brane system is related with the system of D3-branes in the toric Calabi-Yau cone by T-duality along the 57 directions. It is possible to obtain information about gauge theories such as anomalies, marginal deformations, etc. by studying corresponding fivebrane systems [5 – 7].

We can generalize the brane systems by introducing extra ingredients. The introduction of fractional D3-branes in the Calabi-Yau set-up can be realized in the fivebrane system by assigning integers representing D5-brane charges to external lines in the web-diagram [8, 5]. This changes each asymptotic part of the NS5-brane into D5-NS5 bound state. The D5-brane charge conservation requires the numbers of D5-branes on faces change depending on the numbers assigned to external lines, and this gives different ranks of SU($N$) factors in the gauge group. It can be shown that the gauge anomaly cancels when the D5-brane charge conserves [5].

We can also introduce flavor branes, which give fields belonging to the fundamental and the anti-fundamental representations. In [9] non-compact D7-branes wrapped on divisors in toric Calabi-Yau cones are investigated, and the matter contents which these flavor branes give rise to are proposed. Such flavor D7-branes are dual to D5-branes spreading along 012346 directions in the fivebrane systems. We discuss this type of flavor branes in section 5 and extend the results in [9].

Recently, orientifolds of brane tilings are investigated in [10]. There are several possibilities of orientifold planes which preserve $\mathcal{N} = 1$ supersymmetry. In [10], O5-planes, fixed points in bipartite graphs, and O7-planes, fixed lines in graphs, are investigated, and simple prescription to obtain field contents are given. The orientations of these orientifold planes are given in table 2. They also propose a set of rules which uniquely determines the $\mathbb{Z}_2$ orientifold parity of mesonic operators when the positions of fixed points in the bipartite graphs and their "charges" are specified. In this paper, we concentrate on the orientifold

with O5-planes, and derive these rules from the viewpoint of fivebrane systems. We leave the O7-plane case for future work.

If we construct the gauge theory for an orientifolded fivebrane system by the naive orientifold projection, the daughter theory, the theory obtained by the projection from the parent theory, in general possesses gauge anomalies. This can be cured by introducing an appropriate number of fundamental or anti-fundamental representation fields, which we call quarks. A purpose of this paper is to explain how these extra quark fields arise from the viewpoint of fivebrane system. By analogy to the relation between the gauge anomaly cancellation and the D5-brane charge conservation in the un-orientifolded case, it is natural to expect the emergence of the fundamental representation in the orientifolded brane tilings is also guaranteed by the D5-brane charge conservation. We will show that this is actually the case.

For this to happen it is important that O5-planes carry the D5-brane charge, and its signature changes when it intersects with NS5-branes [11 – 14]. As is shown in section 3 this property of O5-planes explains how the quark fields arise. At the same time, this fact raises a problem. When we use the rules proposed in [10] we have to specify "charges" of the four fixed points. These charges, however, cannot be identified with the RR-charges of orientifold planes because an O5-plane carries both positive and negative RR-charges if it intersects with NS5-branes. We need to distinguish the RR-charges of O5-planes and "charges" used in the rules. In this paper, in order to distinguish them from RR-charges of O5-planes, we refer to the "charges" in the rules as "transposition parities" or, simply, "T-parities", because they are directly related to the symmetry of the corresponding field under the transposition.[1] To clarify the relation between the T-parity and the RR-charge of O5-planes is another purpose of this paper.

This paper is organized as follows. In the next section, we briefly review the rules proposed in [10]. In section 3 we discuss anomaly cancellations, and we there give an explanation for the emergence of (anti-)fundamental fields which cancels the gauge anomaly from the viewpoint of fivebrane systems. In section 4 we discuss the relation between $\mathbb{Z}_2$ parity of mesonic operators and the RR-charges of O5-planes, which may depend on the position on the O5-planes. This gives rules to determine $\mathbb{Z}_2$ parity from the RR charges of O5-planes. By comparing these rules and those in [10] we relate the RR-charge and the T-parity. We investigate the relation between flavor branes and quark fields in section 5, and propose superpotentials which correctly reproduce the worldvolumes of flavor D7-branes in the Calabi-Yau cones as the loci in which quarks become massless. Section 6 is devoted for discussions.

## 2. T-parity and mesonic operators

In this section we briefly review the rules to determine the theories realized on orientifolded brane tilings proposed in [10]. We here only discuss orientifold with O5-planes, which are represented as four fixed points on the torus.

[1] Unfortunately, this name is the same as the T-parity in the little Higgs models [15]. We hope no confusion will arise.



JHEP03(2008)058

In the parent theory, each face represents an SU($N$) factor in the gauge group. If a face is identified with another face by the orientifolding, we should identify the corresponding two SU($N$). Let SU($N$) and SU($N$)$'$ be a pair of two factors identified. The reversal of orientation of open strings implies that these two factors should be identified via the charge conjugation. Namely, upper and lower indices of SU($N$) correspond to lower and upper indices of SU($N$)$'$, respectively. The bi-fundamental field $\Phi^a{}_{b'}$ with one upper SU($N$) index $a$ and one lower SU($N$)$'$ index $b'$, which exists if two faces identified are adjacent with each other, is regarded as field $\Phi^{ab}$ with two upper SU($N$) indices or $\Phi_{a'b'}$ with two lower SU($N$)$'$ indices. The symmetry for two indices of these fields is determined according to the following rule proposed in [10].

**Rule 1** (Edge rule)**.** *If a fixed point with positive/negative T-parity is on an edge, the field associated with the edge belongs to the symmetric/antisymmetric representation.*

If a face is identified with itself by the orientifolding, the corresponding gauge group SU($N$) becomes $Sp$ or $SO$ group according to the rule [10]:

**Rule 2** (Face rule)**.** *If a fixed point with positive/negative T-parity is inside a face, SO/Sp gauge group lives on the face.*

Because the orientifold flip exchanges white and black vertices, fixed points cannot be at vertices.

The two rules above are rules for fields which are mapped to themselves by the orientifold flip. The orientifold transformations of other elementary fields, which are mapped to other fields, depend on how we define the relative phases of fields. In [10], instead of giving such transformations for elementary fields, they give rules for gauge invariant mesonic operators, which are defined as the trace of product of bi-fundamental fields. On the brane tiling, such mesonic operators are described as closed paths made of arrows corresponding to the constituent bi-fundamental fields. The $\mathbb{Z}_2$ parity of a mesonic operator is determined by combining the following rules:

**Rule 3** (Product rule)**.** *The $\mathbb{Z}_2$ parity of a mesonic operator corresponding to $\mathbb{Z}_2$ symmetric path passing through two fixed points is the product of the T-parities of the fixed points.*

**Rule 4** (Superpotential rule)**.** *The $\mathbb{Z}_2$ parity of a mesonic operator appearing in the superpotential is negative.*

For later convenience we introduce the following expression for product rule:

$$P[\mathcal{O}] = \int_C T, \tag{2.1}$$

where $T = \left[\begin{smallmatrix} t_4 & t_3 \\ t_1 & t_2 \end{smallmatrix}\right]$ are the set of four T-parities of four O5-planes on $\mathbb{T}^2$, whose positions are shown in figure 2, and $\int_C$ represents the product of two parities assigned to fixed points passed through by a $\mathbb{Z}_2$ symmetric path $C$. In section 4, we clarify the relation between T-parity and RR-charge by using $\mathbb{Z}_2$ parity obtained by these rules.

As a corollary of the rules above, we can show that the following sign rule imposed on the T-parities of the orientifold planes [10].



JHEP03(2008)058

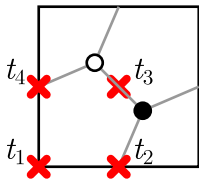


**Figure 2:** In the O5-plane case, we have four fixed points on $\mathbb{T}^2$. The notation $T = \begin{bmatrix} t_4 & t_3 \\ t_1 & t_2 \end{bmatrix}$ is meant to represent T-parities of four orientifold planes, as shown in this figure.

**Rule 5** (Sign rule)**.** *The product of all the T-parities is equal to* $(-1)^{N_W/2}$ *where* $N_W$ *is the number of the terms in the superpotential, which is equal to the number of vertices in the bipartite graph.*

## 3. Anomaly cancellation

With fivebrane systems described by brane tilings, we can realize quiver gauge theories with different ranks depending on faces by changing the numbers of D5-branes depending on faces. The D5-brane charge conservation requires that when the numbers of two adjacent faces are not the same, the difference must be canceled by the inflow of the charge from the NS5-brane corresponding to edges. In the un-orientifolded case, it can be shown [5] that the gauge anomaly cancels if the brane system is consistent with the D5-brane charge conservation law.

The purpose of this section is to show that this is the case for orientifolded brane tilings. The gauge group of an orientifolded theory consists of $\mathrm{SU}(N)$, $\mathrm{SO}(N)$, and $\mathrm{Sp}(N/2)$ factors. (When we consider gauge group $\mathrm{Sp}(N/2)$, we always assume that $N$ is an even integer.) If a face does not have fixed point inside it or on its boundary the anomaly cancellation are guaranteed in the same way as the un-orientifolded case by the D5-brane charge conservation. In the following we discuss anomaly cancellation for a face with an O5-plane inside it or on its boundary.

### 3.1 O5-planes inside faces

If a face has a fixed point inside it and is identified with itself by the orientifold projection, the gauge group realized on the face is $SO$ or $Sp$. These groups do not have the ordinary gauge anomaly. We should, however, take care of the Witten's anomaly [16] for $Sp$ gauge groups. The cancellation of Witten's anomaly requires the number of fundamental representations for each $Sp$ group must be even. We can easily show that this condition automatically holds if the D5-charge conservation law is satisfied in the brane system.

Because black vertices are mapped to white vertices by the orientifold flip, a face with O5-plane inside it has $4n + 2$ edges. For concreteness let us consider an example of a hexagonal face shown in figure 3 (a). Generalization to other cases is trivial. If the T-parity of the fixed point is negative $\mathrm{Sp}(N/2)$ gauge group lives on the hexagonal face at the center. The face is enclosed by six edges. Only three of them are independent and the other three are mirror images. When we consider anomaly, only bi-fundamental fields for



JHEP03(2008)058

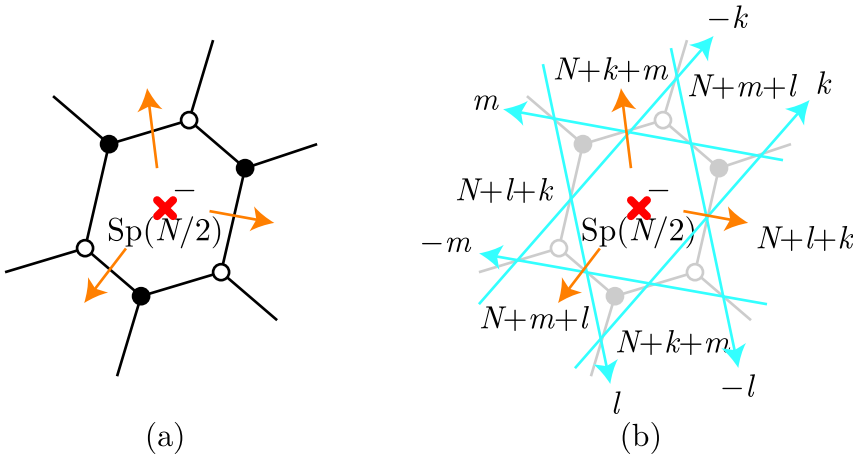


**Figure 3:** A face with fixed point inside it. The independent bi-fundamental fields are shown as outgoing arrows.

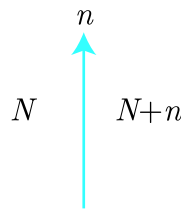


**Figure 4:** The D5-brane charges assigned to two adjacent faces and the edge between them are shown.

the independent three edges should be taken into account. We can, for example, take three outgoing arrows as independent bi-fundamental fields.

When we discuss fivebrane charge conservation, it is convenient to use diagrams in which zig-zag paths are represented as smooth cycles going on the right/left side of black/white vertices in the zig-zag path. (Figure 3 (b)) We call such diagrams *fivebrane diagrams*. (These are the same as what are referred to as "rhombus loop diagrams" in [17])

When the numbers of D5-branes on faces are different, the difference of the D5-branes charge must be supplied by the attached NS5-branes, which are represented as cycles in the diagram. In order to assign charges to faces in a consistent way with the D5-brane charge conservation, we first assign D5-charges to cycles, and the charges of faces are determined so that if we go across a cycle from one face to another, the D5-charges of the faces change by the charge assigned to the cycle. In our convention, if up-going cycle carries charge $n$ and $N$ is assigned to the face on the left side, the number assigned to the right is $N + n$. (Figure 4) Two cycles which are mirror to each other must have the same D5-charges with opposite sign because the orientifold flip reverses the orientation of the cycles. The charges of six adjacent faces are shown in figure 3. The numbers of Sp($N/2$) fundamental



JHEP03(2008)058

representations for three independent arrows are

$$N_1 = N + k + m, \quad N_2 = N + m + l, \quad N_3 = N + l + k. \tag{3.1}$$

Because $N$ is an even integer, the total number $N_1 + N_2 + N_3 = 3N + 2k + 2m + 2l$ is also an even integer, and the Witten's anomaly does not arise.

### 3.2 O5-planes on edges

When an orientifold plane is on an edge of a bipartite graph, two SU($N$) gauge groups on both sides of the edge are identified, and the bi-fundamental field coupling to these two gauge groups becomes symmetric or antisymmetric representation of the SU($N$) gauge group. The anomaly coefficient $d_R$ for these tensor representations are given by

$$d_{\begin{smallmatrix}\square\\\square\end{smallmatrix}} = (N-4)d_{\square}\,, \quad d_{\square\!\square} = (N+4)d_{\square}\,. \tag{3.2}$$

These are different from the contribution $Nd_{\square}$ of the bi-fundamental field in the parent theory, and we need extra ingredient in order to cancel the gauge anomaly. The simplest way to cancel this anomaly is to introduce four fundamental or anti-fundamental chiral multiplets as is pointed out in [10].

How these new matter fields arise in the brane system? A natural way to introduce these (anti-)fundamental fields is to introduce four flavor branes. If we introduce four D5-branes coinciding with the O5-plane, we may obtain four fundamental fields. (This cannot be directly shown by quantizing open strings due to the complicated structure of the brane system.) However, this answer is not satisfactory. On the gauge theory side, we must introduce four (anti-)fundamental representations so that the anomaly cancels. Otherwise the theory would be inconsistent. On the other hand, at first sight, it seems possible to introduce an arbitrary number of flavor branes. Note that we do not have to require the cancellation of RR-charge carried by the O5-plane. Because some of transverse directions of the O5-plane is non-compact, the RR-flux induced by O5-plane and flavor branes can escape to infinity. The RR-flux may cause the breaking of conformal symmetry, but it does not cause any inconsistency at all.

Moreover, the RR-charge of O5-plane (which are defined as integral of flux over $RP^3$, not over $S^3$) is $\pm 1$, and the number of D5-branes including mirror images required to cancel the O5-charge is 2. Even if we introduced flavor D5-branes which cancel the O5-charge, we do not obtain the desired number of fundamental representations.

The key to solve this puzzle is the fact that in our brane system O5-planes and NS5-branes co-exist, and when an O5-plane intersects with NS5-branes it changes its RR-charge [11 – 14]. In the brane system we consider here an O5-plane is a two dimensional plane in 4567 space. Its worldvolume is spread along non-compact 46 directions. The NS5-branes are also two dimensional surfaces, and if corresponding cycle, zig-zag path, on the tiling goes through the fixed point, it shares one direction with the O5-plane.

Let us consider the conifold case as an example. The fivebrane diagram is given in figure 5 (a). $a$, $b$, $c$, and $d$ are O5-planes and the cycles $\mu$, $\nu$, $\rho$, and $\sigma$ are NS5-branes.

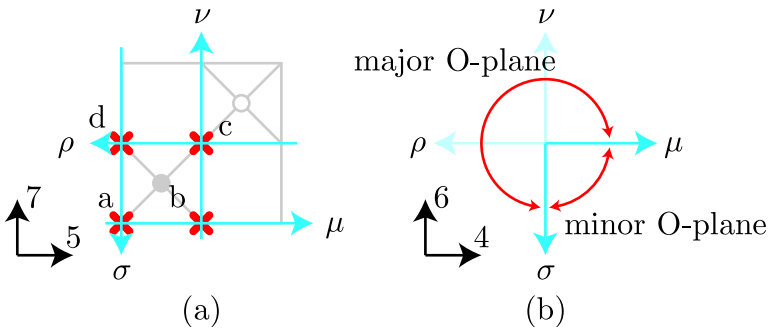


**Figure 5:** The example of the conifold. Here we show $\mathbb{T}^2$ (57) directions. $\mu$, $\nu$, $\rho$, $\sigma$ are cycles of NS5-branes and $a, b, c, d$ are intersection points of O5-planes with D5.

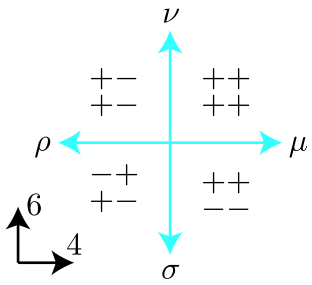


**Figure 6:** RR-charges of four O5-planes. RR-charge assignment changes when crossing NS5-brane cycles $(\mu, \nu, \rho, \sigma)$ and thus depends on quadrants on 46-plane.

Each of them spreads along the following directions in 4567 space:

$$a, b, c, d : 46, \quad \mu, \rho : 45, \quad \nu, \sigma : 67. \tag{3.3}$$

We see that, for example, the O5-plane $a$ and the NS5-brane $\mu$ share one direction $x^4$, and they intersect along a line. The O5-plane $a$ also intersects with NS5-brane $\sigma$ along a line. As a result, the O5-plane $a$ is divided into two parts by the two NS5-branes $\mu$ and $\sigma$. On the 46-plane, these two parts are represented as one quadrant and the rest (figure 5 (b)). In general an O5-plane at an intersection of two cycles in a fivebrane diagram is divided into two parts by two legs in the web-diagram. We call these two parts minor and major O5-planes according to their central angles. Because the RR-charge of the O5-plane changes when it intersects with NS5-branes, the minor and major O5-planes for the same fixed point have opposite RR-charges to each other. This is the case for other three orientifold planes, $b$, $c$, and $d$ in the conifold example, and the RR-charge assignments to the four orientifold planes depend on quadrants on 46-plane. One example is shown in figure 6.

Now let us take account of the RR-charge conservation. The simplest way to satisfy the conservation law is to introduce four (including mirror images) D5-branes on top of $O5^-$-plane compensating the change of O5-plane's RR-charge at the intersection of O5 and NS5 (figure 7). With the assumption of the gauge anomaly cancellation, we expect one of



JHEP03(2008)058

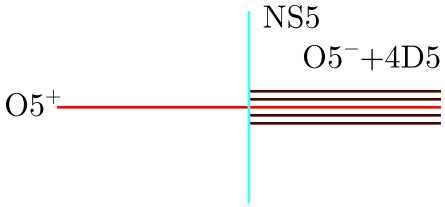


**Figure 7:** When O5-brane intersects with NS5-brane, its RR-charge changes its sign.Moreover, in order to conserve RR-charge, inclusion of four flavor D5-branes (including their mirrors) on top of O5-plane are required.

the following two combinations arise at the O5-plane.

$$\text{positive T-parity} : \square\!\!\square + 4\,\square \ , \quad \text{negative T-parity} : \square\square + 4\,\overline{\square} \ . \tag{3.4}$$

More generally we can introduce more flavor branes spreading over whole 46-plane. It is also possible to transfer the excess of RR charge as a flow on the NS5-brane, and put flavor branes off the O5-planes. These possibilities are discussed in section 5.

## 4. Relation to Calabi-Yau cones

### 4.1 Orientifold of general toric CY cones

The purpose of this subsection is to establish the relation between the RR-charge of O5-planes and the $\mathbb{Z}_2$ parity of mesonic operators with the help of the T-duality between fivebrane systems and Calabi-Yau cones.

**Toric diagram.** Let us start from a toric Calabi-Yau cone $\mathcal{M}$ described by a toric diagram. In this paper we only consider three-dimensional Calabi-Yau manifolds. Let $v_i \in \Gamma = \mathbb{Z}^3$ be the set of lattice points in the toric diagram. By $\mathrm{SL}(3,\mathbb{Z})$ transformation, we can take the coordinate system in which the components of $v_i$ are given by

$$v_i = (p_i, q_i, 1). \tag{4.1}$$

The toric diagram is usually represented as a two-dimensional diagram by using the first two components of these vectors. An example of $\mathbb{C}^3$ case is shown in figure 8 (a).

We define the dual cone $\mathcal{C}^*$ as the set of vectors $w \in \mathbb{R}^3$ satisfying

$$v_i \cdot w \geq 0 \quad \forall i. \tag{4.2}$$

When we consider resolutions of the toric Calabi-Yau, Kähler parameters come to the right hand side of this inequality. In this paper we will not discuss such resolutions and the right hand side is always zero. In such a case we do not have to use all $v_i$ to define $\mathcal{C}^*$ by (4.2), and we only need $v_\alpha$ corresponding to the corners of the toric diagram. Here notation $\alpha, \beta \ldots$ is used to denote lattice points in the corners of toric diagram, and $i, j \ldots$ denotes all the lattice points in the toric diagram. We further assume that the label $\alpha$

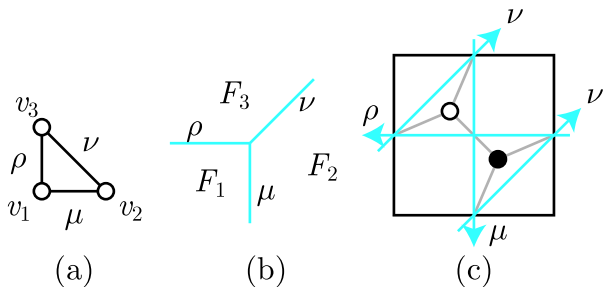


**Figure 8:** Shown here are toric diagram (a), web-diagram (b), and bipartite graph with fivebrane diagram (c) for $\mathbb{C}^3$.

increases one by one as we go around the perimeter of toric diagram in counterclockwise manner. The boundary of the dual cone $\partial\mathcal{C}^*$ consists of flat faces called facets. Each facet corresponds to each vector $v_\alpha$, and is defined as the set of points satisfying $v_\alpha \cdot w = 0$ and $v_\beta \cdot w \geq 0 \ \ (\forall \beta \neq \alpha)$. We denote the facet corresponding to $v_\alpha$ by $F_\alpha$. The structure of the base manifold $\mathcal{C}^*$ is conveniently expressed as a planar diagram by projecting the facets onto a two-dimensional plane by simply neglecting the third coordinate. It is called a web-diagram. Figure 8 (b) is an example of web-diagram for $\mathbb{C}^3$. The lines in the web-diagram represent the edges of the base manifold $\mathcal{C}^*$.

We can regard the Calabi-Yau manifold as the $\mathbb{T}^3$ fibration over the dual cone $\mathcal{C}^*$ (4.2), although strictly speaking some cycles of $\mathbb{T}^3$ shrinks on facets as we will explain. Let $(\phi_1, \phi_2, \phi_3)$ be the coordinates in the toric fiber. We choose the period of each coordinate to be $2\pi$. We can regard $\Gamma$ as the lattice associated with the toric fiber $\mathbb{T}^3$. Namely, we can associate points in $\Gamma$ with cycles in $\mathbb{T}^3$. By this identification, we can regard an arbitrary non-vanishing vector $v \in \Gamma$ as a generator of $\mathrm{U}(1)$ isometry of the $\mathbb{T}^3$. We denote the symmetry generated by $v$ by $\mathrm{U}(1)[v]$. Two flavor symmetries which do not rotate the supercharges are $\mathrm{U}(1)[(1,0,0)]$ and $\mathrm{U}(1)[(0,1,0)]$, and R-symmetry is $\mathrm{U}(1)[(a_1, a_2, 1)]$. When $a_1$ and $a_2$ are appropriately chosen this gives the R-symmetry in the superconformal algebra [18].

On a facet $F_\alpha$ the cycle specified by $v_\alpha$ in $\mathbb{T}^3$ fiber shrinks and the fiber becomes $\mathbb{T}^2$. In order to parameterize the $\mathbb{T}^2$ fiber on each facet, the following coordinate change is convenient.

$$(\phi_1, \phi_2, \phi_3) = \theta_1(1,0,0) + \theta_2(0,1,0) + \theta_3(p_i, q_i, 1). \tag{4.3}$$

This is equivalent to

$$\theta_1 = \phi_1 - p_\alpha \phi_3, \quad \theta_2 = \phi_2 - q_\alpha \phi_3, \quad \theta_3 = \phi_3. \tag{4.4}$$

On the facet, the $\theta_3$-cycle shrinks and $(\theta_1, \theta_2)$ is a pair of good coordinates on $\mathbb{T}^2$. By taking T-duality along these two angular coordinates we obtain fivebrane system described by the brane tiling. The third angular coordinate $\theta_3$ is identified with the argument of the complex coordinate $x^8 + ix^9$ in the fivebrane system.



JHEP03(2008)058

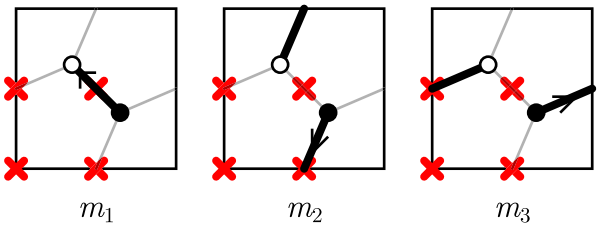


**Figure 9:** The three perfect matchings for the bipartite graph of $\mathbb{C}^3$ are shown.

**Perfect matchings and zig-zag paths.** A perfect matching is a subset of edges of a bipartite graph such that for each vertex one (and only one) of the edges ending on the vertex is included in the subset. Figure 9 shows the three perfect matchings for $\mathbb{C}^3$. Perfect matchings plays important roles in the connection between bipartite graphs and Calabi-Yau geometry. See [19] for review. Given a perfect matching, we can define the corresponding unit flow by regarding each matched edge as black-to-white flow by one. A unit flow is a flow with source 1 at each black vertex and sink 1 at each white vertex. Flows corresponding to perfect matchings are special kind of unit flows. We abuse the term "perfect matchings" in the following to mean also the corresponding unit flows. The difference of two unit flows is a conserved flow. For such conserved flows we can uniquely define the flux across closed cycles. For a flow $f$ and a cycle $C$, we denote the total flux of $f$ across $C$ by $\langle f, C\rangle$. We define this flux so that if $C$ is an up-going cycle $\langle f, C\rangle$ is the flux of $f$ passing $C$ from left to right. The set of two fluxes across $\boldsymbol{\alpha}$ and $\boldsymbol{\beta}$-cycles is called height change, and we denote it by $h(f)$.

$$h(f) = (\langle f, \boldsymbol{\alpha}\rangle, \langle f, \boldsymbol{\beta}\rangle). \tag{4.5}$$

(We take the $\boldsymbol{\alpha}$ and $\boldsymbol{\beta}$-cycles along $x^5$ and $x^7$, respectively. Also, in this paper we use bold letters to denote $\boldsymbol{\alpha}$ and $\boldsymbol{\beta}$-cycles in order to distinguish them from $\alpha, \beta, \ldots$, which are labels of corners of the toric diagram.)

Let us label perfect matchings by indices $\alpha'$, $\beta'$, .... We can define "relative positions" between two perfect matchings $m_{\alpha'}$ and $m_{\beta'}$ by the height change $h(m_{\alpha'} - m_{\beta'})$, and we can plot matchings as points on a two-dimensional lattice. An important fact is that this set of points is nothing but the toric diagram [1, 20]. By this fact we can associate each vertex in the toric diagram with perfect matchings. In the $\mathbb{C}^3$ example, the matchings $m_1$, $m_2$, and $m_3$ in figure 9 correspond to the facets $F_1$, $F_2$, and $F_3$, respectively of figure 8 (b). (We use the term "facets" not only for faces of dual cones but also for their projection onto the web diagrams.) In general several perfect matchings may be associated with one vertex. For a vector $v_i$ in the toric diagram, let $m[v_i]$ be one of the associated matchings. Then the following relation holds:

$$h(m[v_i] - m[v_j]) = v_i - v_j. \tag{4.6}$$

This equation makes sense because the third component of $v_i - v_j$ always vanishes and gives a vector in the two-dimensional lattice. Also, even though we have in general several



JHEP03(2008)058

perfect matchings associated with vertices $v_i$ and $v_j$, this equation holds regardless of the choice of perfect matchings $m[v_i]$ and $m[v_j]$.

There are some arguments that there are bipartite graphs which do not give physical quiver gauge theories [17]. To obtain meaningful gauge theories we need to impose the condition that there is one and only one perfect matching associated for each corner in toric diagrams. In the following we only consider such "good" bipartite graphs. We denote the unique perfect matching for a corner $\alpha$ by $m_\alpha$. This one-to-one correspondence between corners of the toric diagram and perfect matchings of the bipartite graph plays important roles in what follows.

For a general vector $v \in \mathbb{Z}^3$, we define $m[v]$ in the following way. First we decompose $v$ into linear combination of $v_i$ as $v = \sum_i a_i v_i$ with integral coefficients $a_i$. Then $m[v]$ is defined by

$$m[v] = \sum_i a_i m[v_i]. \tag{4.7}$$

The source at black vertices and sink at white vertices of the flow $m[v]$ are always the same, and it is equal to the sum of the coefficients, $\sum_i a_i$. This is nothing but the third component of $v$, and thus independent of how to decompose $v$ into $v_i$. One should note that if $v$ is on the plane of toric diagram $m[v]$ gives a unit flow. Again there are ambiguities in $m[v]$ associated with the choice of perfect matching $m[v_i]$ for each $v_i$ and in the way of decomposing $v$ into $v_i$. The difference of two different choices of $m[v]$, however, is always a conserved flow with vanishing height change, and this ambiguity does not matter in the following arguments.

**Shrinking cycles and NS5-branes.** By the T-duality along $\theta_1$ and $\theta_2$, edges of the base manifold $\mathcal{C}^*$, or, equivalently, external lines in the web-diagram are transformed into NS5-branes wrapped on cycles in the dual $\mathbb{T}^2$. The winding number of each NS5-brane is determined in the following way. Let us focus on the edge of $\mathcal{C}^*$ shared by adjacent two facets $F_\alpha$ and $F_{\alpha+1}$. This edge is given as the set of points satisfying

$$v_\alpha \cdot w = 0, \quad v_{\alpha+1} \cdot w = 0. \tag{4.8}$$

By taking the difference of these two conditions, we obtain

$$(\Delta p, \Delta q) \cdot (w_1, w_2) = 0, \tag{4.9}$$

where $\Delta p = p_{\alpha+1} - p_\alpha$, $\Delta q = q_{\alpha+1} - q_\alpha$, and $w_1$ and $w_2$ are the first two components of the vector $w$. Namely, the external line in the web-diagram is a line perpendicular to the side between the corners $v_\alpha$ and $v_{\alpha+1}$ of the toric diagram.

Let $(\theta_1, \theta_2)$ be the coordinate of $\mathbb{T}^2$ fiber on the facet $F_\alpha$.[2] These coordinates are inert under the isometry $\mathrm{U}(1)[v_\alpha]$. In order to examine the behavior of the $\mathbb{T}^2$ fiber near the external line shared by $F_\alpha$ and $F_{\alpha+1}$, let us consider the action of $\mathrm{U}(1)[v_{\alpha+1}]$ on the $\mathbb{T}^2$. The Killing vector $v_{\alpha+1}$ for the adjacent facet $F_{\alpha+1}$ acts on the coordinate $(\theta_1, \theta_2)$ as

$$\theta_1 \to \theta_1 + \Delta p\ t, \quad \theta_2 \to \theta_2 + \Delta q\ t, \tag{4.10}$$

[2]We have chosen this notation for simplicity, although strictly speaking we should write $(\theta_1^\alpha, \theta_2^\alpha)$ since these coordinates depend to $\alpha$.

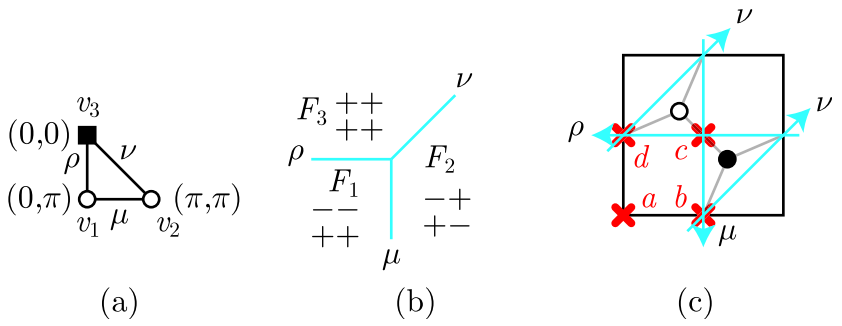


**Figure 10:** Some diagrams for $\mathbb{C}^3$ orientifold are shown. (a) shows the toric diagram. The square box shows the choice of $(2\mathbb{Z})^2$ sublattice, and the number placed at each vertex represents shift variable $(\pi s_1, \pi s_2)$ on the facet corresponding to each vertex. (b) shows the web-diagram, together with the assignment of RR-charges on each facet. Note RR-charges change when crossing cycles of NS5-branes, just as in the case of conifold shown in figure 6. (c) shows the bipartite graph, and $a, b, c, d$ denotes the position of O5-planes.

with a parameter $t$. The corresponding cycle, $(\Delta p, \Delta q)$-cycle, shrinks at the boundary between $F_\alpha$ and $F_{\alpha+1}$. By the T-duality transformation along $\theta_1$ and $\theta_2$, this shrinking cycle is transformed to NS5-brane wrapped on $(\Delta q, -\Delta p)$-cycle. In the bipartite graph, these cycles wrapped by the NS5-branes are represented as the zig-zag paths. (See figure 8 (c). There cycles of NS5-branes are denoted by $\mu, \nu, \rho$.)

**Orientifold.** Let us consider orientifold $\mathcal{M}/\mathbb{Z}_2$. We only consider $\mathbb{Z}_2$ which is a subgroup of the $\mathrm{U}(1)^3$ isometry of $\mathcal{M}$. As we see below this type of $\mathbb{Z}_2$ gives orientifolded fivebrane systems with O5-planes, which we are interested in. We can specify the $\mathbb{Z}_2$ action by specifying a Killing vector $V$ for $\mathrm{U}(1)$ symmetry which include the $\mathbb{Z}_2$ as its subgroup. Without loss of generality we assume that $V$ is a primitive vector in the integral lattice. The generator of $\mathbb{Z}_2$ is given by

$$(\phi_1, \phi_2, \phi_3) \to (\phi_1, \phi_2, \phi_3) + \pi V. \tag{4.11}$$

Two vectors $V$ and $V'$ with components different by even integers define the same $\mathbb{Z}_2$. Since $\phi_3$ is identified with the argument of the coordinate $x^8 + ix^9$, third component of $V$ is 1 (modulo 2). This means that the vector $V$ can be represented as a point on the toric diagram. In order to define the orientifold we only need to specify the first two components of $V$ mod 2. This is graphically represented in toric diagram by choosing $(2\mathbb{Z})^2$ lattice. When we draw the toric diagram of an orientifolded toric Calabi-Yau, we will use squares to represent points in the $(2\mathbb{Z})^2$ lattice while other points are represented as circles. An example of such a toric diagram for an orientifold of $\mathbb{C}^3$ is given in figure 10 (a). We have four choices of sublattice $(2\mathbb{Z})^2$, but in this example, three of them are equal up to $\mathrm{SL}(2,\mathbb{Z})$ transformation, so only one of them is shown. The other possible choice of $(2\mathbb{Z})^2$ will be shown later in figure 11.

From the $\mathbb{Z}_2$ action on $\phi_i$ given in (4.11), together with definition of $\theta$ in (4.4), we can



JHEP03(2008)058

easily obtain the following action on the $\mathbb{T}^2$ fiber on each facet as

$$(\theta_1, \theta_2) \to (\theta_1 - \pi s_1, \theta_2 - \pi s_2), \tag{4.12}$$

with the shift variables $s_1$ and $s_2$ on each facet given by

$$s_\alpha = v_\alpha - V. \tag{4.13}$$

Note that the shift depends on facets $F_\alpha$, and this formula can be used to determine the shift for each facet. In the example in figure 10 (a), the shift of the $\mathbb{T}^2$ fiber in each facet is given beside the corresponding vertex.

**T-duality of orientifolds.** In order to relate a toric Calabi-Yau cone to a fivebrane system, we define Cartesian-like coordinate as follows. Let $x^4$ and $x^6$ be coordinates parameterizing $\partial\mathcal{C}^*$, the plane of web-diagram, and $\rho \geq 0$ be the "distance" from the boundary $\partial\mathcal{C}^*$. We do not need precise form of these coordinates because we are only interested in the topological structure. We combine $\rho$ and $\phi_3$ to define $x^8$ and $x^9$ by $x^8 + ix^9 = \rho e^{i\phi_3}$. The coordinates $x^4$, $x^6$, $x^8$, and $x^9$ defined above are identified with the same coordinates in the fivebrane system, while $\theta_1$ and $\theta_2$ are the dual coordinates to the compact coordinates $x^5$ and $x^7$. The $\mathbb{Z}_2$ action on these coordinates is given by

$$(x^4, \theta_1, x^6, \theta_2, x^8, x^9) \to (x^4, \theta_1 - \pi s_1, x^6, \theta_2 - \pi s_2, -x^8, -x^9). \tag{4.14}$$

If both $s_1$ and $s_2$ are even integers, there is a codimension-2 fixed plane, O7-plane. Otherwise, there is no fixed plane.

By the T-duality along the compact coordinates $\theta_1$ and $\theta_2$, the orientifold is transformed to another orientifold with the geometric $\mathbb{Z}_2$ action

$$(x^4, x^5, x^6, x^7, x^8, x^9) \to (x^4, -x^5, x^6, -x^7, -x^8, -x^9). \tag{4.15}$$

This is the orientifold of the fivebrane systems which we discuss in this paper. This orientifold has four O5-planes at $(x^5, x^7) = (0, 0)$, $(\pi, 0)$, $(0, \pi)$, and $(\pi, \pi)$. There is no dependence on $(s_1, s_2)$ in the geometric $\mathbb{Z}_2$ action (4.15).

The information of $s_1$ and $s_2$ is encoded in the RR-charges of four O5-planes. If both $s_1$ and $s_2$ are even integers, there is an O7-plane on the Calabi-Yau side, and the dual configuration contains four O5-planes with the same sign of RR-charge as the O7-plane. Otherwise, we have no O7-plane on the Calabi-Yau side, and two $\mathrm{O5}^+$ and two $\mathrm{O5}^-$ in the fivebrane system at the position depending on $(s_1, s_2)$ [21]. The relation between $(s_1, s_2)$ and the charges of O5-planes are summarized below.

$$(s_1, s_2) = (0, 0) : \left[\begin{smallmatrix} + & + \\ + & + \end{smallmatrix}\right] \text{ or } \left[\begin{smallmatrix} - & - \\ - & - \end{smallmatrix}\right], \tag{4.16}$$

$$(s_1, s_2) = (1, 0) : \left[\begin{smallmatrix} + & - \\ + & - \end{smallmatrix}\right] \text{ or } \left[\begin{smallmatrix} - & + \\ - & + \end{smallmatrix}\right], \tag{4.17}$$

$$(s_1, s_2) = (1, 1) : \left[\begin{smallmatrix} + & - \\ - & + \end{smallmatrix}\right] \text{ or } \left[\begin{smallmatrix} - & + \\ + & - \end{smallmatrix}\right], \tag{4.18}$$

$$(s_1, s_2) = (0, 1) : \left[\begin{smallmatrix} + & + \\ - & - \end{smallmatrix}\right] \text{ or } \left[\begin{smallmatrix} - & - \\ + & + \end{smallmatrix}\right]. \tag{4.19}$$



JHEP03(2008)058

By the T-duality relations (4.16-4.19) we define the map $\sigma$ from charge assignments $Q$ to $(\mathbb{Z}_2)^2$ valued vector $s$,

$$\sigma : Q \to s \tag{4.20}$$

If we use the notation of (2.1), then explicit expression for $s = \sigma(Q)$ is given by

$$(-1)^{s_1} = \int_{\boldsymbol{\alpha}} Q, \quad (-1)^{s_2} = \int_{\boldsymbol{\beta}} Q. \tag{4.21}$$

Here $\boldsymbol{\alpha}$ (resp. $\boldsymbol{\beta}$) denotes $\mathbb{Z}_2$-symmetric $\alpha$-cycle (resp. $\boldsymbol{\beta}$-cycle) of $\mathbb{T}^2$ which passes through two O5-planes. We have two such $\mathbb{Z}_2$-symmetric $\boldsymbol{\alpha}$-cycles (resp. $\boldsymbol{\beta}$-cycles), but both of these two gives the same answer, because the product of all four charges is always $+1$. The relations in (4.21) show that we can regard $(s_1, s_2)$ as the relative charges among four RR charges.

For two charge assignments $Q_1 = \left[\begin{smallmatrix} q_{14} & q_{13} \\ q_{11} & q_{12} \end{smallmatrix}\right]$ and $Q_2 = \left[\begin{smallmatrix} q_{24} & q_{23} \\ q_{21} & q_{22} \end{smallmatrix}\right]$, we define their product by componentwise multiplication:

$$Q_1 \cdot Q_2 = \left[\begin{smallmatrix} q_{14}q_{24} & q_{13}q_{23} \\ q_{11}q_{21} & q_{12}q_{22} \end{smallmatrix}\right]. \tag{4.22}$$

Then you can directly verify the formula

$$\sigma(Q_1 \cdot Q_2) = \sigma(Q_1) + \sigma(Q_2) \bmod 2. \tag{4.23}$$

If we are given the geometric action of $\mathbb{Z}_2$ on a Calabi-Yau cone, we obtain $(s_1, s_2)$, which can be regarded as relative charges of O5-planes, on each facet by the relation (4.13). Conversely, given relative charges, we always have two possible charge assignments as listed in (4.16)–(4.19), which are related to each other by total charge flip. We cannot choose one of them only with the information of the geometric action of $\mathbb{Z}_2$.

Instead of starting from the geometric $\mathbb{Z}_2$ action on the Calabi-Yau, let us assume that we are given a brane tiling with fixed points specified, and that we know charge distribution on one facet. With this information, we can reconstruct all the information about fivebrane system and $\mathbb{Z}_2$ action on the Calabi-Yau cone in the following way.

We first reconstruct the toric diagram and the web-diagram by using zig-zag paths. Let $F_\alpha$ and $F_{\alpha+1}$ be two adjacent facets. If the side between two corners $v_\alpha$ and $v_{\alpha+1}$ includes $n$ edges, there are $n$ parallel zig-zag paths corresponding to the external lines between facets $F_\alpha$ and $F_{\alpha+1}$. Let $Z_{\alpha+1,\alpha}$ be the union of these $n$ zig-zag paths.

If the charge assignment $Q_\alpha = \left[\begin{smallmatrix} q_{\alpha 4} & q_{\alpha 3} \\ q_{\alpha 1} & q_{\alpha 2} \end{smallmatrix}\right]$ in the facet $F_\alpha$ is given, we can determine $Q_{\alpha+1}$ in the next facet $F_{\alpha+1}$ by flipping the RR-charges of fixed points which are passed through by $Z_{\alpha+1,\alpha}$.

This relation between $Q_\alpha$ and $Q_{\alpha+1}$ is expressed as

$$Q_{\alpha+1} = Q_\alpha \cdot \rho(Z_{\alpha+1,\alpha}). \tag{4.24}$$

Here $\rho(Z_{\alpha+1,\alpha})$ is the charge assignment such that if a fixed point is on a zig-zag path in $Z_{\alpha+1,\alpha}$, the charge of the fixed point is $-1$ while the charge is 1 otherwise.

Let us take the orientifold of $\mathbb{C}^3$ shown in figure 10 as an example. By using the bipartite graph (c), we can draw the corresponding toric diagram and web-diagram. The



JHEP03(2008)058

toric diagram has three corners and correspondingly there are three facets in the web-diagram. We assume that we know the charge distribution on one of the facets, say, $F_1$. The charge assignments on other facets are determined as follows. If we move from $F_1$ to $F_2$ on the web-diagram, we cross the NS5-brane $\mu$. The figure 10 (c) shows that this NS5-brane intersects with O5-plane $b$ and $c$. and we can obtain the charge assignment on $F_2$ from that on $F_1$ by flipping the RR-charges of $b$ and $c$. More formally, we have $Q_1 = \left[\begin{smallmatrix} - & - \\ + & + \end{smallmatrix}\right]$, $Q_2 = \left[\begin{smallmatrix} - & + \\ + & - \end{smallmatrix}\right]$, and $\rho(Z_{2,1}) = \left[\begin{smallmatrix} + & - \\ + & - \end{smallmatrix}\right]$, and this satisfies the relation (4.24). By repeating this procedure, we obtain charge assignments on all the facets.

The relation (4.24) is consistent with the relation (4.13). In order to see this, we use the following relation, which is proved in appendix A.1:

$$\sigma(\rho(Z_{\alpha+1,\alpha})) = h(Z_{\alpha+1,\alpha}) \bmod 2. \tag{4.25}$$

By using (4.6), (4.23), and (4.25) the relation (4.24) is mapped by $\sigma$ to

$$s_{\alpha+1} - s_\alpha = v_{\alpha+1} - v_\alpha, \tag{4.26}$$

and this shows that the relation (4.24) is "integrable", and consistently determine the vector $V$ modulo 2.

**$\mathbb{Z}_2$ parity of mesonic operators.** Mesonic operators in a gauge theory are represented as closed paths in the brane tiling. Let $C[\mathcal{O}]$ be the closed path corresponding to a mesonic operator $\mathcal{O}$. Mesonic operators are important when we relate gauge theories and toric Calabi-Yau cones because we can regard mesonic operators as holomorphic monomial functions in the Calabi-Yau cone. In other words, we can use (an appropriate subset of) mesonic operators as coordinates in the Calabi-Yau. To establish the relation between mesonic operators and monomial functions in the toric Calabi-Yau, we can use charges associated with $\mathrm{U}(1)^3$ symmetry. For both mesonic operators and monomial functions we can assign three charges, and by these charges we can establish one-to-one correspondence between mesonic operators and monomial functions.

As we mentioned above, we can specify $\mathrm{U}(1)$ symmetry by a vector $v \in \Gamma$. We can determine the charges of mesonic operators for a given $\mathrm{U}(1)$ by the following relation

$$\mathrm{U}(1)[v] \text{ charge of an operator } \mathcal{O} = \langle m[v], C[\mathcal{O}] \rangle, \tag{4.27}$$

where $\langle f, C \rangle$ is the flux of $f$ across $C$ defined above (4.5). Because the path for a gauge invariant mesonic operator is closed, the ambiguity in the definition of $m[v]$ does not affect the flux.

As a special case of this relation, the $\mathbb{Z}_2$ parity of a mesonic operator $\mathcal{O}$ under the transformation (4.11) can be obtained from the $\mathrm{U}(1)[V]$ charge of the mesonic operator. If the charge is even (odd), the parity is + (−). In other words, we can determine the $\mathbb{Z}_2$ parity $P[\mathcal{O}]$ for an operator $\mathcal{O}$ by the mod 2 flux of the unit flow $m[V]$ across $C[\mathcal{O}]$.

$$P[\mathcal{O}] = (-1)^{\langle m[V], C[\mathcal{O}] \rangle}. \tag{4.28}$$

We refer to the unit flow $m[V]$ as a parity flow.



JHEP03(2008)058

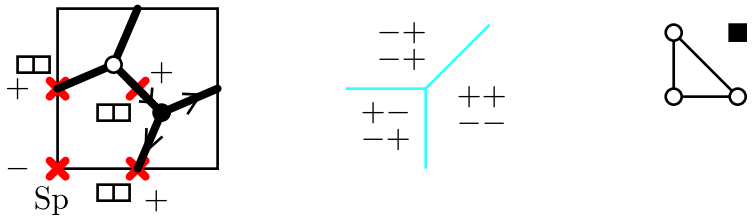


**Figure 11:** Another example of orientifold of $\mathbb{C}^3$ is shown. See also figure 10. In this case the square vertex is not contained in the lattice points of the toric diagram, and the parity flow is obtained as a linear combination of perfect matchings.

If the toric diagram includes square vertices, we can use one of perfect matchings associated with one of square vertices in the toric diagram as a parity flow. Otherwise, we have to use linear combination of perfect matchings. One such example is shown in figure 11.

### 4.2 T-parity and RR-charge

The purpose of this subsection is to clarify the relation between the T-parity and the RR-charge by comparing the formula (4.28) for $\mathbb{Z}_2$ parity obtained in the previous subsection and the rules proposed in [10].

**Superpotential rule.** We can easily reproduce the superpotential rule (Rule 4) from the formula (4.28). Because terms in the superpotential correspond to cycles enclosing only one vertex in a bipartite graph, the rule is equivalent to the statement that the $\mathbb{Z}_2$ parity of a mesonic operator $\mathcal{O}$ is given by the flux of an odd flow, flow with odd source and sink at each vertex, across the path $C[\mathcal{O}]$. Because $m[V]$ is a unit flow it correctly gives the $\mathbb{Z}_2$ parity satisfying the superpotential rule.

**Product rule.** Next we are going to reproduce the product rule (Rule 3). Let us define $\rho(m_\alpha)$ as the charge assignment such that if a fixed point is on the perfect matching $m_\alpha$ the charge of the fixed point is $-1$, while the charge is $+1$ otherwise. This definition is similar to that of $\rho(Z_{\alpha+1,\alpha})$, and we have the following relation:

$$\rho(Z_{\alpha+1,\alpha}) = \rho(m_{\alpha+1}) \cdot \rho(m_\alpha). \tag{4.29}$$

In order to understand this relation, recall (4.6) says

$$m_{\alpha+1} - m_\alpha = Z_{\alpha+1,\alpha} \bmod (\text{boundaries}), \tag{4.30}$$

since winding numbers, or height function of both sides of this equation coincides. By definition, this almost proves (4.29). The only remaining problem is the possible contribution to $\rho$ from boundary terms, which are conserved flows with vanishing height change. Namely, boundaries might pass through fixed points and contribute to $\rho$. It turns out, however, that this contribution is absent since it is impossible for boundaries to pass through fixed points and be $\mathbb{Z}_2$-symmetric at the same time. This proves (4.29).



JHEP03(2008)058

Now if we use (4.29), we can rewrite the relation (4.24), which represents the RR-charge flip of O5-planes at intersections with NS5-branes, into the following form:

$$Q_{\alpha+1} \cdot \rho(m_{\alpha+1}) = Q_\alpha \cdot \rho(m_\alpha). \tag{4.31}$$

This relation means that $Q_\alpha \cdot \rho(m_\alpha)$ in fact does not depend on facets, and it is possible to define facet-independent charge $T'$ by

$$T' = Q_\alpha \cdot \rho(m_\alpha). \tag{4.32}$$

We propose the charge assignment $T'$ defined by this equation is nothing but the T-parity $T$.

For this charge $T'$ to be acceptable as the T-parity, we should confirm that $T'$ defined in (4.32) combined with the formula (2.1) gives the same $\mathbb{Z}_2$ parity as (4.28) for mesonic operators which are described by $\mathbb{Z}_2$ symmetric cycles. This can be easily shown by rewriting the formula (4.28) in terms of $T'$. We first use (4.13) and rewrite (4.28) as

$$P[\mathcal{O}] = (-1)^{\langle m_\alpha, C[\mathcal{O}]\rangle}(-1)^{\langle m[s_\alpha], C[\mathcal{O}]\rangle}. \tag{4.33}$$

In the appendix A.1, we prove the following two formulae:

$$(-1)^{\langle m_\alpha, C[\mathcal{O}]\rangle} = \int_{C[\mathcal{O}]} \rho(m_\alpha), \tag{4.34}$$

and

$$(-1)^{\langle m[s_\alpha], C[\mathcal{O}]\rangle} = \int_{C[\mathcal{O}]} Q_\alpha, \tag{4.35}$$

where $\int_{C[\mathcal{O}]}$ means the product of charges of fixed points passed through by the path $C[\mathcal{O}]$, as defined in (2.1). The first says that if $m_\alpha$ is the perfect matching for $\alpha$, which is $\mathbb{Z}_2$ symmetric, and if $C[\mathcal{O}]$ is a $\mathbb{Z}_2$ symmetric path, only the fixed points contribute to the mod 2 intersection number. Substituting (4.34) and (4.35) into (4.33) we immediately obtain

$$P[\mathcal{O}] = \int_{C[\mathcal{O}]} T', \tag{4.36}$$

and this is nothing but the formula (2.1) with $T$ replaced by $T'$.

Note that not only $T = T'$ but also $T = -T'$ give the same $\mathbb{Z}_2$ parity of mesonic operators, and we still have the following two possibilities:

$$T = \pm T'. \tag{4.37}$$

In order to determine the overall sign of the T-parity, we need additional information, or assumption about the relation between overall sign of RR-charge and overall sign of T-parity.

The reason why we cannot simply identify RR-charges and T-parities is that as we mentioned above the RR-charge may change depending on the facets. This is, however, only the case for the O5-planes on edges. If an O5-plane is inside a face, its RR-charge is everywhere the same, and we can simply identify the RR-charge as T-parity. So, let us adopt the following assumption:



JHEP03(2008)058

- For fixed points on faces, the T-parity is the same as the RR-charge of the O5-plane.

If there exist fixed points on faces, this condition uniquely determine the T-parity as

$$T = T' = Q_\alpha \cdot \rho(m_\alpha). \tag{4.38}$$

There is a simple relation among RR-charge and T'-charge of O5-planes. The definition (4.32) of $T'$ can in fact be rewritten in the following form which does not directly refer to perfect matchings:

**Rule 6** (Angle rule)**.**

*When O5-plane consists of two parts with opposite RR-charges, the $T'$ charge of the O5-plane is the same as the RR-charge of the O5-plane occupying the major angle.*

This can be shown from (4.32) and the following theorem proved in the appendix A.3:

**Theorem 1.** *Let $I$ be an edge in a bipartite graph, and $\{F_\alpha, F_\beta, \ldots, F_\gamma\}$ be the set of facets whose associated perfect matchings include the edge $I$. Then, facets in the set $\{F_\alpha, F_\beta, \ldots, F_\gamma\}$ form one continuous region in the web-diagram, and the central angle of the region is always a minor angle.*

The angle rule (Rule 6) shows that the $T'$-charge of an O5-plane is determined by the local information about the O5-plane without using charges of other orientifold planes. If we assume this is the case for the T-parity, it is natural that the T-parity for a fixed point is always determined by (4.38) regardless of the existence of O5-planes inside faces.

In the next section, we give another reason why we should choose the overall sign of T-parity as the equation (4.38).

## 5. Flavor branes

### 5.1 Quark mass terms

In the previous section we discussed only the mesonic operators made of bi-fundamental fields. Let us turn to quark fields in the (anti-)fundamental representation, which emerge when we introduce flavor branes.

We here only discuss flavor D5-branes parallel to the O5-planes in table 1. In this subsection we do not consider orientifolds. By T-duality transformation they are transformed into D7-branes wrapped on divisors in the toric Calabi-Yau geometry. In [9] graphical representation of such flavor D7-branes and corresponding superpotential terms are proposed. A D7-brane wrapped on a divisor in the Calabi-Yau 3-fold is represented as a curve connecting two punctures on the NS5-brane worldvolume, which is referred to as Riemann surface in [9]. In fivebrane diagrams, these two punctures are represented as two cycles, and the curve connecting two punctures corresponding to an intersection of these cycles. This intersection point is nothing but the flavor D5-brane worldvolume projected onto the 57-plane.

On the web-diagram, a flavor brane is represented as a fan between two external legs corresponding to the two zig-zag paths (figure 12(a)). When we specify two legs, there



JHEP03(2008)058

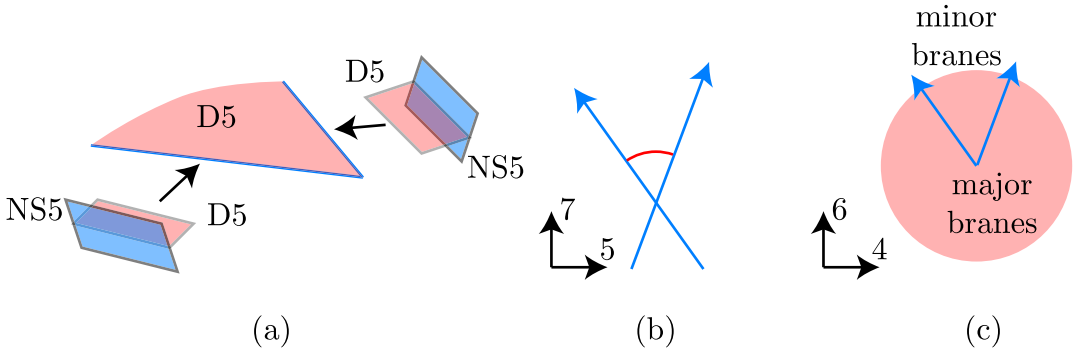


**Figure 12:** (a) shows a flavor brane stretched between two legs in a web-diagram. In the internal 57-space, the D5-brane is attached to the NS5-branes. In the corresponding fivebrane diagram (b) we use an arc to represent the flavor brane. As is shown in (c) there are two possible flavor branes associated with a pair of legs in the web-diagram. We call them minor and major branes.

are always two fans defined by these legs. One has minor central angle and the other has major central angle. We call corresponding two possible flavor branes for a given pair of external legs minor branes and major branes (figure 12(c)). In order to distinguish these two types of flavor branes in fivebrane systems, we represent flavor branes as arcs at the intersection of cycles (figure 12(b)). Arcs are drawn in the angles corresponding to the fans on the web-diagram. We can define these angles because the directions of the cycles are the same as the directions of external legs in the web-diagram.

**Minor flavor branes.** In [9] the following superpotential is proposed for quarks $q$ and $\widetilde{q}$ emerging by the introduction of flavor branes placed on an intersection $I$:

$$W = \widetilde{q}\Phi_I q, \tag{5.1}$$

where $\Phi_I$ is the bi-fundamental field associated with the intersection $I$. This superpotential corresponds only to minor flavor branes as will be confirmed in the following.

If we assume that quark fields are supplied from D3-D7 strings in the Calabi-Yau perspective, the fundamental fields must become massless when D3-branes coincide with the D7-branes. Namely, massless loci of quark fields in the moduli space should be identified with the worldvolume of the D7-branes. (In this paper we consider only the Coulomb branch, in which quarks have vanishing vevs.)

When the quark mass term is given by (5.1), the massless locus is given by $\Phi_I = 0$. (Following the usual procedure to obtain Calabi-Yau geometry, we here treat all the gauge groups as U(1)). In order to determine the corresponding divisor in the moduli space, we should solve the F-term conditions imposed on bi-fundamental fields. The solution is given by [20]

$$\Phi_I = \prod_{\alpha' \ni I} \rho_{\alpha'}, \tag{5.2}$$

where $\rho_{\alpha'}$ are complex fields defined for each perfect matching $\alpha'$, and $\alpha' \ni I$ means that the product is taken over all the perfect matchings which include the edge $I$. By this



JHEP03(2008)058

relation we can describe the moduli space of quiver gauge theory as the moduli space of gauged linear sigma model (GLSM) with the fields $\rho_{\alpha'}$. The equation (5.2) means that the massless locus is given by the union of loci defined by $\rho_{\alpha'} = 0$. Because we are interested in divisors, we do not take care of subspace of moduli space with dimension less than 2. We only focus on the submanifold $\mathcal{M}' \subset \mathcal{M}$ which is defined as the complement of the submanifold corresponding to the legs and the center of the web-diagram. We can show that in this submanifold GLSM fields $\rho_{\alpha'}$ which do not correspond to corners of the toric diagram do not vanish. This allow us to forget about such fields and we have only to take care of fields $\rho_\alpha$, which correspond to corners in the toric diagram. The following theorem can be proved:

**Theorem 2.** *In the subspace $\mathcal{M}'$, the divisor corresponding to a facet $F_\alpha$ is given by $\rho_\alpha = 0$ in the GLSM.*

The proof is given in appendix A.2. With this theorem we obtain

$$\text{massless locus} = \bigcup_{\alpha \ni I} F_\alpha, \tag{5.3}$$

where we use $F_\alpha$ for the divisor corresponding to the facet. The theorem 1 means that this is nothing but the worldvolume of the minor branes associated with the edge $I$.

**Major flavor branes.** In order to obtain the worldvolume of major flavor branes, we need different quark mass terms from (5.1). Let us assume the following form of quark mass terms:

$$W = \widetilde{Q}\mathcal{O}Q, \tag{5.4}$$

where $\mathcal{O}$ is composite operator made of bi-fundamental fields. We denote quark fields provided by major flavor branes by $Q$ and $\widetilde{Q}$ while we write $q$ and $\widetilde{q}$ the quark fields for minor branes. From the theorem 1, the worldvolume of major flavor branes associated with the edge $I$ is given by

$$\text{major branes} = \bigcup_{\alpha \not\ni I} F_\alpha. \tag{5.5}$$

where $\alpha \not\ni I$ means that the product is taken over all the perfect matchings which do not include the edge $I$ and are associated with corners of the toric-diagram. By the theorem 2 this is given by $\mathcal{O} = 0$ with the operator $\mathcal{O}$ defined by

$$\mathcal{O} = \prod_{\alpha' \not\ni I} \rho_{\alpha'}. \tag{5.6}$$

In order to write the superpotential (5.4), we need to rewrite the operator $\mathcal{O}$ in terms of bi-fundamental fields in the gauge theory. It is easy to see that

$$\mathcal{O} = \prod_{J \in k, J \neq I} \Phi_J, \tag{5.7}$$



JHEP03(2008)058

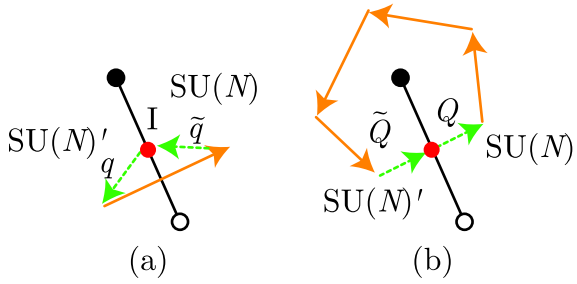


**Figure 13:** Closed paths representing quark mass terms for minor flavor branes (a) and major flavor branes (b) are shown.

| | $\mathrm{SU}(N) \times \mathrm{SU}(N)'$ |
|---|---|
| bi-fund. | $\Phi^i_{Ij'}(\square\,, \overline{\square}\,)$ |
| minor brane | $q^{i'}(1, \square\,)$, $\widetilde{q}_i(\overline{\square}\,, 1)$ |
| major brane | $Q^i(\square\,, 1)$, $\widetilde{Q}_{i'}(1, \overline{\square}\,)$ |

**Table 3:** The representations of quark fields for two types of flavor branes are shown.

where $k$ is one of two endpoints of the edge $I$, and $J \in k$ means edges sharing the vertex $k$ as their endpoints. When we regard this as the operator in the gauge theory with non-Abelian gauge group the constituent fields should be ordered so that the color indices of adjacent fields match. The operator $\mathcal{O}$ is graphically represented as the path consisting of solid arrows in figure 13(b). In the definition of the operator $\mathcal{O}$ there are two choices of the endpoint of the edge $I$. Let $\mathcal{O}_B$ and $\mathcal{O}_W$ be the two operators obtained by choosing black and white endpoints of $I$, respectively. Because the superpotential of bi-fundamental fields includes

$$W = \mathrm{tr}(\Phi_I \mathcal{O}_B) - \mathrm{tr}(\Phi_I \mathcal{O}_W), \tag{5.8}$$

and the F-term condition of $\Phi_I$ gives

$$\mathcal{O}_B = \mathcal{O}_W, \tag{5.9}$$

the superpotential (5.4) does not depend on the choice between $\mathcal{O}_B$ and $\mathcal{O}_W$.

Let us compare the superpotentials (5.1) for minor branes and (5.4) for major branes.

$$W_{\text{minor}} = \widetilde{q}_i \Phi^i_{Ij'} q^{j'}, \quad W_{\text{major}} = \widetilde{Q}_{i'} \mathcal{O}^{i'}{}_j Q^j. \tag{5.10}$$

These two are represented as cycles made of dashed and solid arrows in figure 13. In (5.10) color indices are explicitly written. Notice that the existence of these terms requires the chirality of the quark fields should be opposite between minor and major flavor branes. If we have a bi-fundamental field in the representation $(\square\,, \overline{\square}\,)$ at the edge $I$, minor branes give quarks in the representation $(\overline{\square}\,, 1)$ and $(1, \square\,)$ while major branes give ones in $(\square\,, 1)$ and $(1, \overline{\square}\,)$ (table 3). This difference is important when we use flavor branes to cancel the gauge anomaly associated with orientifold planes. In figure 14, the difference of quark representations is expressed by the orientation of dashed arrows.



JHEP03(2008)058

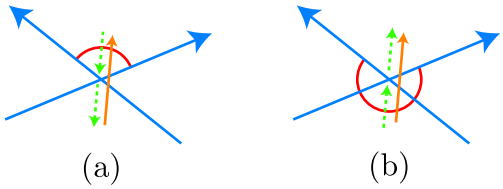


**Figure 14:** Graphical representation of minor branes (a) and major branes (b), and corresponding fields are shown.

| | SU($N$) | SO($k+4$) | Sp($k/2$) |
|---|---|---|---|
| $\Phi$ | $\square\square$ | 1 | 1 |
| $q$ | $\bar{\square}$ | $\square$ | 1 |
| $Q$ | $\square$ | 1 | $\square$ |

**Table 4:** Fields arising at the fixed point with positive T-parity are shown. SU($N$) is the gauge group and SO($k+4$) $\times$ Sp($k/2$) is the flavor symmetry.

### 5.2 Orientifold planes and flavor branes

As we mentioned in section 3, if an O5-plane is divided into major and minor O5-planes these two parts carry opposite RR-charges to each other. One way to compensate the charge flip of O5-planes is to introduce appropriate number of flavor branes coinciding with the O5-planes. Another way to realize the charge conservation using RR-charge flow along NS5-branes is discussed in the next subsection.

Let us first consider the case with positive T-parity. In this case, by the angle rule (Rule 6) with $T'$ identified with $T$, the minor and major O5-planes carry negative and positive RR-charges, respectively. We can match the RR-charges of minor and major parts by introducing $k+4$ minor branes and $k$ major branes. In the parent theory these flavor branes provide quarks shown in table 3. By the orientifold projection, the two gauge groups SU($N$) and SU($N$)$'$ on the both sides of the edge $I$ are identified, and the bi-fundamental field $\Phi^i_{Ij'}$ in ( $\square$ , $\bar{\square}$ ) representation becomes field $\Phi_I^{\{ij\}}$ in the symmetric representation $\square\square$ of SU($N$). The quark fields $q$ and $\widetilde{q}$, and $Q$ and $\widetilde{Q}$ are identified, and independent fields are $q$ in $\bar{\square}$ and $Q$ in $\square$ . (Table 4)

The superpotential is given by

$$W_{(T=+)} = \delta_{AB} q_i^A \Phi^{\{ij\}} q_j^B + J_{CD} Q^{Ci} \mathcal{O}_{ij} Q^{Dj}, \tag{5.11}$$

where $\mathcal{O}$ is the composite operator defined in the parent theory by (5.7). The flavor symmetry is SO($k+4$) $\times$ Sp($k/2$), and $\delta_{AB}$ and $J_{CD}$ are the symmetric and antisymmetric invariant tensors of the flavor groups SO($k+4$) and Sp($k/2$), respectively.

The fields arising at the fixed point contribute to the SU($N$) gauge anomaly by

$$d_{\square\square} + (k+4) d_{\bar{\square}} + k d_{\square} = N d_{\square}\,, \tag{5.12}$$



JHEP03(2008)058

| | SU($N$) | SO($k+4$) | Sp($k/2$) |
|---|---|---|---|
| $\Phi$ | $\square\square$ | 1 | 1 |
| $q$ | $\bar{\square}$ | 1 | $\square$ |
| $Q$ | $\square$ | $\square$ | 1 |

**Table 5:** Fields arising at the fixed point with negative T-parity are shown. SU($N$) is the gauge group and SO($k+4$) $\times$ Sp($k/2$) is the flavor symmetry.

and this is the same as the contribution of the bi-fundamental field in the parent theory. Therefore, if the parent theory is anomaly free before the introduction of flavor branes, the daughter theory is also automatically anomaly free.

If the T-parity is negative, the minor and major O5-planes carry positive and negative RR-charges, respectively. We can match the RR-charges of two parts by introducing $k$ minor and $k+4$ major flavor branes. In the parent theory, in addition to the bi-fundamental field in ( $\square$ , $\bar{\square}$ ), we have quark fields shown in table 3. By the orientifold projection, these fields become an antisymmetric tensor field $\Phi^{[ij]}$ in $\begin{smallmatrix}\square\\\square\end{smallmatrix}$ , $q$ in $\bar{\square}$ , and $Q$ in $\square$ . The flavor symmetry is SO($k+4$) $\times$ Sp($k/2$). The gauge and flavor quantum numbers are shown in table 5.

The superpotential is given by

$$W_{(T=-)} = \delta^{AB} q_A^i \mathcal{O}_{ij} q_B^j + J^{CD} Q_{Ci} \Phi^{[ij]} Q_{Bj}. \tag{5.13}$$

As well as the case of positive T-parity, the fields arising at the fixed point contribute the SU($N$) gauge anomaly by the same amount as the bi-fundamental field in the parent theory

$$d_{\begin{smallmatrix}\square\\\square\end{smallmatrix}} + (k+4) d_{\square} + k d_{\bar{\square}} = N d_{\square}\,, \tag{5.14}$$

and the anomaly cancels if so does the anomaly in the parent theory before introducing the flavor branes.

Note that in the above we assumed that $T = +T'$ when we use Rule 6 to determine the RR-charge of minor and major O5-planes. If we take the opposite sign $T = -T'$, the chirality of quark fields arising at the fixed points are reversed, and the gauge anomaly does not cancel. This is another reason why we should take $T = +T'$.

### 5.3 Flow of flavor brane charge

In the previous subsection we discuss the relation between RR charge conservation and gauge anomaly cancellation in the case of orientifold. We show that if there are appropriate number of flavor branes coinciding with O5-planes the gauge anomaly cancels. The requirement of the existence of flavor branes coinciding with O5-planes, however, is too restrictive. We can loosen this condition by using the flow of the D5-brane charge along NS5-branes.

Let us first consider un-orientifolded case. As an example let us suppose that we introduce $N_f$ minor branes at an edge $I$. In general we need to introduce more flavor branes to realize the charge conservation and the gauge anomaly cancellation. A simple way is

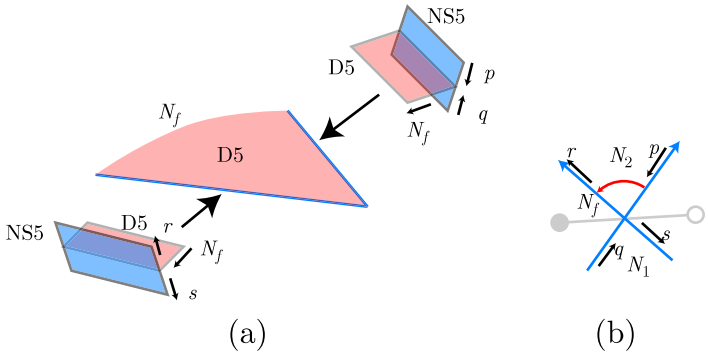


**Figure 15:** D5-brane charge carried by one NS5-brane is transfered into another NS5-brane by flavor D5-branes. The charge conservation requires $p + q = N_f = r + s$.

to introduce the same number of major flavor branes at the same edge. Then the quark spectrum becomes vector-like and the gauge anomaly cancels. The charge conservation of flavor branes is also obvious. This is, however, not the unique way to fulfill these consistency conditions.

Look at figure 15. It shows $N_f$ minor flavor branes between two external legs in the web-diagram. These flavor branes carry D5-brane charge $N_f$, and the charge is supplied from one of the NS5-branes and flows into another NS5-brane on the other side. Even if we do not introduce major flavor branes at the edge $I$, the D5-charge can flow on NS5-branes, and it can be consistently conserved if we arrange the flow in the network of NS5-branes appropriately. In the example shown in figure 15, the following charge conservation condition must hold:

$$p + q = N_f = r + s, \tag{5.15}$$

where $p$, $q$, $r$, and $s$ are the D5-charges flowing on NS5-branes as shown in figure 15.

The flow of the D5-brane charge on NS5-branes are graphically described as flows along cycles in fivebrane diagrams. At intersections, these D5-charges can be transfered from one cycle to another, and the amount of the transfered charge is determined by the numbers of the minor and major flavor branes. The direction of the charge transfer is represented as arrows on the arcs in the diagram. The supersymmetry requires these arrows are always in the same direction because a flow in the opposite direction means that the corresponding flavor branes carry negative RR-charge. We take the convention in which all the arcs are counter-clockwise.

The charge carried by cycles must be taken into account when we determine the charge of color D5-branes, the numbers assigned to faces in the bipartite graph. The number assigned to each face in a fivebrane diagram must be determined so that the difference of numbers assigned to adjacent faces is equal to the flow along the cycle shared by the faces. See also figure 4. In the example of figure 15 (b), the two numbers $N_1$ and $N_2$ must satisfy

$$N_2 - N_1 = p - s = r - q. \tag{5.16}$$



JHEP03(2008)058

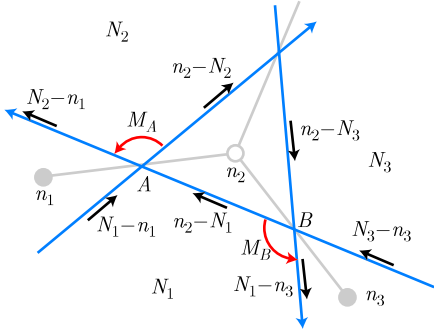


**Figure 16:** The flow on cycles and the transfer at intersections are uniquely determined by the charge assignment to faces.

If the conditions such as (5.15) are satisfied at each intersection, we can consistently determine the charges of faces.

Generalization to orientifolds is straightforward. When we consider charge flow along cycles, we treat a positive O5-plane just like four coincident flavor branes because $O5^+$ transfers the charge by $+2$ from one cycle to another while $O5^-$ transfers charge $-2$ in the opposite direction. We should also impose the $\mathbb{Z}_2$-symmetry on the flow. Because the D5-brane charge does not change its sign by the orientifold flip, the flow of the D5-brane charge should be invariant under the rotation of the diagram by angle $\pi$. See figure 18 for an example.

### 5.4 Charge conservation and anomaly cancellation

In this section we prove that if a fivebrane system respects the D5-brane charge conservation law the gauge anomalies of the corresponding quiver gauge theory cancel.

In order to give a number assignment to faces, cycles, and flavor branes so that the D5-brane charge conserves, we should first assign numbers to faces in fivebrane diagrams. In a fivebrane diagram, there are two kinds of faces: faces corresponding to faces in the bipartite graph and ones corresponding to vertices in the bipartite graph. We assign numbers to both these two types of faces. At this step we have no restriction except that the numbers assigned to faces of the bipartite graph must be non-negative.

Once we assign numbers to faces in the fivebrane diagram, the numbers for each segment in cycles are uniquely determined by the charge conservation law. The number assigned to a part of a cycle shared by two faces is given by the difference of the charges assigned to the two faces. (figure 4)

Finally, after we obtained all the charges assigned to cycles in this way, we determine the charge transfer between two intersecting cycles at every intersection by the charge conservation relation such as (5.15). For the two intersection $A$ and $B$ in figure 16, the flows are

$$M_A = N_1 + N_2 - n_1 - n_2, \quad M_B = N_1 + N_3 - n_2 - n_3. \tag{5.17}$$



JHEP03(2008)058

These numbers gives the difference between numbers of minor and major branes inserted at each intersection.

$$M_A = N_A^{\rm minor} - N_A^{\rm major}, \quad M_B = N_B^{\rm minor} - N_B^{\rm major}. \tag{5.18}$$

It may be convenient to draw arcs for both minor and major flavor branes and assign them the numbers $N^{\rm minor}$ and $N^{\rm major}$ to embed all the information of the brane system in the diagram. In figure 16 we show only the net charge transfer at each intersection.

Let us confirm that the $\mathrm{SU}(N_1)$ anomaly cancels in the example shown in figure 16. The chiral multiplets arising at the intersection $A$ belong to the following representations of gauge group $\mathrm{SU}(N_1) \times \mathrm{SU}(N_2) \times \mathrm{SU}(N_3)$:

$$(\bar{\square}\,, \square\,, 1) + N_A^{\rm minor}[(\square\,, 1, 1) + (1, \bar{\square}\,, 1)] + N_A^{\rm major}[(\bar{\square}\,, 1, 1) + (1, \square\,, 1)] \tag{5.19}$$

These contribute the $\mathrm{SU}(N_1)$ anomaly in the unit of $d_{\square}$ by

$$-N_2 + N_A^{\rm minor} - N_A^{\rm major} = -N_2 + M_A = N_1 - n_1 - n_2. \tag{5.20}$$

At the intersection $B$, we have the following chiral multiplets

$$(\square\,, 1, \bar{\square}\,) + N_B^{\rm minor}[(\bar{\square}\,, 1, 1) + (1, 1, \square\,)] + N_B^{\rm major}[(\square\,, 1, 1) + (1, 1, \bar{\square}\,)], \tag{5.21}$$

and these contribute to the $\mathrm{SU}(N_1)$ anomaly by

$$N_3 - N_B^{\rm minor} + N_B^{\rm major} = N_3 - M_B = -N_1 + n_2 + n_3. \tag{5.22}$$

In the anomalies (5.20) and (5.22), the contributions of $N_2$ and $N_3$ have already canceled. Furthermore, if we add these two contributions (5.20) and (5.22) the contribution of $n_2$ cancels. Similarly, if we sum up all the contribution from corners of the face for the gauge group $\mathrm{SU}(N_1)$, all contributions cancel, and we conclude that number assignments satisfying the D5-brane charge conservation law always give anomaly-free gauge theories.

In the case of orientifolds, we must impose the $\mathbb{Z}_2$ invariance to the numbers assigned to faces. If a number assignment to faces is $\mathbb{Z}_2$ invariant, the other charges assigned to cycles and intersections are also automatically $\mathbb{Z}_2$ invariant. The charge transfer at a fixed point between two cycles intersecting at the fixed point is always even integer. Let $M$ be the charge transfer.

If the T-parity of the O5-plane is positive, the major O5-plane is positive and the minor O5-plane is negative. Because the flow $M$ is the difference of RR-charges of the minor part and the major part, it is given by

$$M = (N_{\rm minor} - 2) - (N_{\rm major} + 2) = N_{\rm minor} - N_{\rm major} - 4, \tag{5.23}$$

where $N_{\rm minor}$ and $N_{\rm major}$ are the numbers of branes coinciding the minor and major O5-planes, respectively. The chiral multiplets arising at the O5-plane and their contribution $d$ to the $\mathrm{SU}(N)$ anomaly are

$$\square\square + N_{\rm major}\,\square + N_{\rm minor}\,\bar{\square}\,, \quad d = (N+4) + N_{\rm major} - N_{\rm minor} = N - M. \tag{5.24}$$

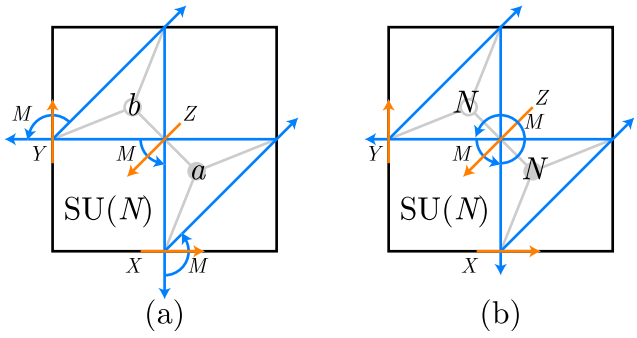


**Figure 17:** Two examples of fivebrane diagrams are shown.

If the T-parity of the O5-plane is negative, the major O5-plane is negative and the minor O5-plane is positive. The charge transfer is given by

$$M = (N_{\text{minor}} + 2) - (N_{\text{major}} - 2) = N_{\text{minor}} - N_{\text{major}} + 4. \tag{5.25}$$

The chiral multiplets and their contribution to the anomaly are

$$\square\!\!\square + N_{\text{major}}\,\square + N_{\text{minor}}\,\overline{\square}\,, \quad d = (N-4) + N_{\text{major}} - N_{\text{minor}} = N - M. \tag{5.26}$$

Because both (5.24) and (5.26) are the same as the anomaly in the parent theory without orientifolding, the anomaly in the orbifold theory cancels if the parent theory with the same number assignment is anomaly free. Therefore, as the un-orbifolded case, a charge conserving number assignment always gives an anomaly-free gauge theory.

### 5.5 Examples

Before ending this section, we give a few examples of fivebrane systems.

Let us first consider the simplest example, $\mathbb{C}^3$ tiling without O5-planes. (figure 17(a)) The fivebrane diagram includes three faces. The hexagonal face with number $N$ being assigned corresponds to gauge group SU($N$). We label the three intersections by $X$, $Y$, and $Z$, and we use the same letters for the corresponding bi-fundamental fields. We assign $a$ and $b$ to the two triangular faces corresponding to the black and white vertices in the bipartite graph. The charge conservation uniquely determines the flow along cycles and the transfer at intersections. The transfer at three intersections are all equal and given by

$$M = 2N - a - b. \tag{5.27}$$

For simplicity let us assume that $M$ is positive and we introduce only minor flavor branes. Then we have the field content in table 6. The superpotential of this theory is

$$W_1 = \text{tr}(XYZ - ZYX) + \text{tr}(\widetilde{q}_X X q_X) + \text{tr}(\widetilde{q}_Y Y q_Y) + \text{tr}(\widetilde{q}_Z Z q_Z). \tag{5.28}$$

By taking T-duality transformation, this system becomes D7-D3 system in $\mathbb{C}^3$. We can identify the diagonal components of $X$, $Y$, and $Z$ as the position of D3-branes. Let us

| | SU($N$) | U($M$)$_X$ | U($M$)$_Y$ | U($M$)$_Z$ |
|---|---|---|---|---|
| $X$, $Y$, $Z$ | adj | 1 | 1 | 1 |
| $q_X$ | $\square$ | $\overline{\square}$ | 1 | 1 |
| $\widetilde{q}_X$ | $\overline{\square}$ | $\square$ | 1 | 1 |
| $q_Y$ | $\square$ | 1 | $\overline{\square}$ | 1 |
| $\widetilde{q}_Y$ | $\overline{\square}$ | 1 | $\square$ | 1 |
| $q_Z$ | $\square$ | 1 | 1 | $\overline{\square}$ |
| $\widetilde{q}_Z$ | $\overline{\square}$ | 1 | 1 | $\square$ |

**Table 6:** The matter content of the gauge theory realized on the fivebrane system figure 17(a).

| | SU($N$) | U($M$) | U($M$)$'$ |
|---|---|---|---|
| $X$, $Y$, $Z$ | adj | 1 | 1 |
| $Q_Z$ | $\square$ | $\overline{\square}$ | 1 |
| $\widetilde{Q}_Z$ | $\overline{\square}$ | $\square$ | 1 |
| $q_Z$ | $\square$ | 1 | $\overline{\square}$ |
| $\widetilde{q}_Z$ | $\overline{\square}$ | 1 | $\square$ |

**Table 7:** The matter content of the gauge theory realized on the fivebrane system in (b) of figure 17. U($M$) and U($M$)$'$ are flavor symmetries realized as gauge symmetry on major and minor flavor branes, respectively.

focus on one of the D3-branes and treat the bi-fundamental fields as complex coordinates in $\mathbb{C}^3$. The massless loci for quarks are given by $X = 0$, $Y = 0$, and $Z = 0$. On the web-diagram these are represented as three facets. The numbers of D7-branes wrapped on the corresponding three divisors are all equal, and given by (5.27). This does not mean that a system with different numbers of D7-branes wrapped on these divisors is inconsistent. For example, it is obviously possible to wrap D7-branes on only one of these divisors. It is just a stack of parallel D7-branes in the flat spacetime. The equality of the numbers of D7-branes on the three divisors is required not for the consistency of the system but for the possibility to transform the system to a fivebrane system. This fact implies that if we want to study all the possible D7-brane configurations in Calabi-Yau cones by means of brane tilings, we need to generalize the brane system by including other kinds of branes.

The second example (figure 17(b)) is $\mathbb{C}^3$ with different flavor branes. We assign all the faces the same number $N$. Then the transfer among cycles at each intersection vanishes. We can, however, introduce the same number of major and flavor branes at each intersection. Let us consider the case with $M$ major and $M$ minor flavor branes at the intersection $Z$. The field content is shown in table 7. The superpotential is given by

$$W_2 = \mathrm{tr}(XYZ - ZYX) + \mathrm{tr}(\widetilde{Q}_Z XY Q_Z) + \mathrm{tr}(\widetilde{q}_Z Z q_Z). \tag{5.29}$$

On the web-diagram, all the three facets are wrapped by $M$ flavor branes. The major branes are wrapped on two facets and the minor branes are wrapped on the other. This means that by taking T-duality we obtain D7-branes wrapped on the same divisor as the



JHEP03(2008)058

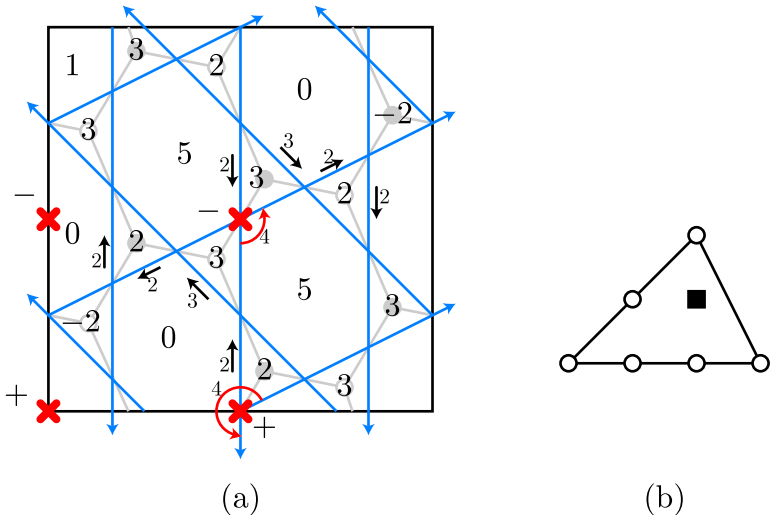


**Figure 18:** A fivebrane realization of the supersymmetric Georgi-Glashow model, which is a famous example of models of dynamical supersymmetry breaking. (a) is the fivebrane diagram and (b) is the corresponding toric diagram.

case of the first example. The difference between two brane configurations is Wilson lines on the D7-branes. In the fivebrane system the position of flavor branes on the $\mathbb{T}^2$ is different. This difference is transformed by the T-duality to the difference of the Wilson lines on the D7-brane worldvolumes. The effect of the Wilson lines may be interpreted as a mass deformation of the theory. We can indeed deform the first example into the second one by adding the following quark mass term to the superpotential (5.28):

$$W_{\text{add}} = -\operatorname{tr}(\widetilde{q}_Y q_X). \tag{5.30}$$

If we eliminate $q_X$ and $\widetilde{q}_Y$ from $W_1 + W_{\text{add}}$ by using the F-term conditions and identify $\widetilde{q}_X$ and $q_Y$ with $\widetilde{Q}_Z$ and $Q_Z$ we obtain the superpotential (5.29) for the second example.

Finally, let us consider an example with O5-planes. As is pointed out in [10], it is easy to make models leading to dynamical supersymmetry breaking by orientifolded brane tilings. As examples they give two brane realizations of the supersymmetric Georgi-Glashow model [22]. Figure 18 shows fivebrane diagrams of one of the models based on $\mathbb{C}^3/\mathbb{Z}_6$ geometry. This fivebrane diagram includes six hexagonal faces with integers 0, 0, 0, 1, 5, and 5 assigned to each. These faces give the gauge group $\mathrm{Sp}(0) \times \mathrm{SU}(0) \times \mathrm{SO}(1) \times \mathrm{SU}(5) \sim \mathrm{SU}(5)$. We also have $\overline{\mathbf{10}}$ from the fixed point at the center and $\mathbf{5}$ from the contacting point of the SU(5) face and the SO(1) face. The D5-brane charge is conserved without introducing any flavor branes, and we have no more extra fields.

## 6. Conclusions and discussions

In this paper we investigated orientifold of brane tilings from the perspective of fivebrane systems. Among several possibilities, we only discussed orientifold with O5-planes which



JHEP03(2008)058

are represented as points in bipartite graphs. We showed that the cancellation of Witten's $\mathbb{Z}_2$ anomaly and gauge anomaly are guaranteed by the conservation of D5-brane charge. The fact that the O5-plane RR-charge flips at the intersection with NS5-brane plays the key role to explain the gauge anomaly cancellation. The charge conservation requires the emergence of appropriate flavor branes, which do not necessarily coincide with the O5-planes, to compensate for the change of the O5-plane charges. These flavor branes provide quark fields which cancel the gauge anomaly generated by symmetric or antisymmetric representation fields.

In section 4 we investigated the relation between fivebrane systems to Calabi-Yau cones. We gave the formula for $\mathbb{Z}_2$ parity of mesonic operators in terms of RR-charges of O5-planes, and establish the relation between RR-charge and T-parity. We also gave quark mass terms which reproduce the world volumes of flavor branes in toric Calabi-Yau cones as the massless loci of quark fields.

All these are quite remarkable, but still there are many open questions.

As we mentioned above, we only investigated the case of orientifold with O5-planes. There are, however, other possibilities with O7-planes. The matter contents for such case is given in [10], and similarly to the O5-brane case, we need fundamental matter fields to cancel gauge anomaly. The emergence of flavor branes should be guaranteed by some consistency in the brane system and it is important to clarify how the quark fields arise in these models.

In section 4.1, we restrict our attention only to RR-charge assignments with positive total charge. (Total charge is the product of RR-charges of four O5-planes.) From the fivebrane perspective, it seems also possible to consider RR-charge assignments with negative total charge. These two possibilities can be distinguished by two $\mathbb{Z}_2$ invariant value of the integral

$$b = \int_{T^2} B_2. \tag{6.1}$$

The invariance under the orientifold flip $b \to -b$ restrict this value to be 0 or $\pi$ mod $2\pi$. As is clarified in [7], this parameter is related to the $\beta$-deformation in the gauge theory. It may be interesting to investigate the relation between the brane configurations with negative total RR-charge and $\beta$-deformation in gauge theories.

In general, the gauge theories realized by the fivebrane systems are not conformal. Such gauge theories without conformal symmetry are known to enjoy phenomenon so-called duality cascade [23]. It is known [24] that type IIA brane construction of $\mathcal{N} = 1$ gauge theories provides simple way to realize Seiberg duality [25] in a geometric way. It would be interesting to study the phenomenon by using the fivebrane systems investigated in this paper.

Construction of models of dynamical SUSY breaking from orientifolded brane tilings is an extremely interesting issue, considering its phenomenological interest. Our analysis clarified the structure of the fivebrane system realizing the model proposed in [10]. We need to consider non-trivial flow of flavor D5-brane charges along NS5-branes. Alternatively, we can use metastable SUSY breaking [26]. In un-orientifolded case it is shown that we have



JHEP03(2008)058

metastable vacuum by the inclusion of flavor branes [9, 27], and we expect existence of metastable vacua in orientifolded case as well.

Finally, it would be interesting to consider application to mirror symmetry for Calabi-Yau orientifolds, since in the un-orientifolded case, brane tilings are quite useful in proving homological mirror symmetry [28 – 30]. We expect several differences, such as that $A_\infty$-structures are replaced by $L_\infty$-structures in orientifold case [31], but the basic line of argument should be similar.

We hope to return to these topics in the future.


## Acknowledgments

We would like to thank F. Koyama for valuable discussions. Y. I. would also like to thank Osaka City University Research Group for Mathematical Physics for the oppertunity of giving a lecture about brane tilings. Y. I. is partially supported by Grant-in-Aid for Young Scientists (B) (#19740122) from the Japan Ministry of Education, Culture, Sports, Science and Technology.




## A. Proofs of theorems

### A.1 Some identifies

In this sections we prove three formulae, originally labeled (4.25), (4.34), and (4.35). The first formula (4.25) is

$$\sigma(\rho(Z_{\alpha+1,\alpha})) = h(Z_{\alpha+1,\alpha}) \bmod 2. \tag{A.1}$$

The second formula (4.34) says if $C$ is a $\mathbb{Z}_2$ symmetric path,

$$(-1)^{\langle m_\alpha, C[\mathcal{O}]\rangle} = \int_{C[\mathcal{O}]} \rho(m_\alpha). \tag{A.2}$$

The final formula (4.35) is

$$(-1)^{\langle m[s_\alpha], C[\mathcal{O}]\rangle} = \int_{C[\mathcal{O}]} Q_\alpha. \tag{A.3}$$

We have renumbered these formulae for convenience.

We first prove (A.2). By definition, $\langle m_\alpha, C[\mathcal{O}]\rangle$ is given by the intersection number of $C[\mathcal{O}]$ with the perfect matching $m_\alpha$. In general, we have many possible intersection points, but if you consider mod 2 intersection number, only intersection points on orientifold planes contribute because other intersection points always come in pairs. We thus have

$$(-1)^{\langle m_\alpha, C[\mathcal{O}]\rangle} = (-1)^{(\text{number of intersection points of } C[\mathcal{O}] \text{ with } m_\alpha \text{ at fixed points})}. \tag{A.4}$$

The r.h.s. is nothing but the definition of $\int_{C[\mathcal{O}]} \rho(m_\alpha)$, which proves (A.2).

Now the proof of other formulae are easy. (A.1) is shown from (A.2) as follows:

$$\begin{aligned}(-1)^{\sigma(\rho(Z_{\alpha+1,\alpha}))_1} &= \int_{\boldsymbol{\alpha}} \rho(Z_{\alpha+1,\alpha}) \quad (\because\ (4.21)) \\ &= \int_{\boldsymbol{\alpha}} \rho(m_{\alpha+1}) \int_{\boldsymbol{\alpha}} \rho(m_\alpha) \quad (\because\ (4.29)) \\ &= (-1)^{\langle m_{\alpha+1}, \boldsymbol{\alpha}\rangle}(-1)^{\langle m_\alpha, \boldsymbol{\alpha}\rangle} \quad (\because\ (A.2) \text{ with } C[\mathcal{O}] = \boldsymbol{\alpha}\text{-cycle}) \\ &= (-1)^{\langle Z_{\alpha+1,\alpha}, \boldsymbol{\alpha}\rangle} \quad (\because\ (4.30)) \\ &= (-1)^{h(Z_{\alpha+1,\alpha})_1} \quad (\because\ (4.5)).\end{aligned} \tag{A.5}$$

(The subscripts 1 mean the first component of the vectors.)

Similarly, when $C[\mathcal{O}]$ is the $\boldsymbol{\alpha}$-cycle, we have

$$\begin{aligned}(-1)^{\langle m[s_\alpha], C[\mathcal{O}]\rangle} &= (-1)^{\langle m[s_\alpha], \boldsymbol{\alpha}\rangle} \\ &= (-1)^{h(m[s_\alpha])_1} \quad (\because\ (4.5)) \\ &= (-1)^{s_{\alpha 1}} \quad (\because\ (4.6) \text{ and } (4.13)) \\ &= \int_{\boldsymbol{\alpha}} Q_\alpha \quad (\because\ (4.21)).\end{aligned} \tag{A.6}$$

The case of more general $C[\mathcal{O}]$ is similar, and this proves (A.3).

### A.2 Divisors and GLSM fields

We here prove theorem 2. Namely, we show that in the subspace $\mathcal{M}'$ defined in section 5.1 the divisor $F_\alpha$ is given by $\rho_\alpha = 0$, where $\rho_\alpha$ is the GLSM field corresponding to the unique perfect matching $m_\alpha$ for the corner $\alpha$ of the toric diagram. For any perfect matching $m_{\alpha'}$, which does not necessarily correspond to a corner of the toric diagram, there is a corresponding GLSM field $\rho_{\alpha'}$, and in terms of these GLSM fields the solution of the F-term condition is given by [20]

$$\Phi_I = \prod_{\alpha' \ni I} \rho_{\alpha'}, \tag{A.7}$$

where $\alpha' \ni I$ means all perfect matchings including the edge $I$.

The system of $\rho_{\alpha'}$ does not have superpotential and possesses $\mathrm{U}(1)^n$ symmetry, where $n$ is the number of the GLSM fields. Among these $\mathrm{U}(1)$ symmetries, $n-3$ are gauged. The gauged subgroup $\mathrm{U}(1)^{n-3} \subset \mathrm{U}(1)^n$ is specified by the charge matrix $g_k^{\alpha'}$, $k = 1, \ldots, n-3$. The gauge transformation of $\rho_{\alpha'}$ with parameter $\theta_k$ are given by

$$\rho'_{\alpha'} = e^{i\sum_k \theta_k g_k^{\alpha'}} \rho_{\alpha'}. \tag{A.8}$$

By removing unphysical degrees of freedom associated with (complexified version of) this gauge symmetry, we obtain the three dimensional moduli space. We denote the natural map from $\rho$ space $\mathcal{M}_{\mathrm{GLSM}}$ to the three dimensional moduli space $\mathcal{M}$ by $\psi$:

$$\psi : \mathcal{M}_{\mathrm{GLSM}} \to \mathcal{M}. \tag{A.9}$$

These gauge transformation generate shifts in the space of angular variables $\varphi_{\alpha'} = \arg \rho_{\alpha'}$, and the toric fiber $\mathbb{T}^3$ of the moduli space $\mathcal{M}$ can be regarded as classes defined by the following identification relation:

$$\varphi_{\alpha'} \sim \varphi_{\alpha'} + \theta_k g_k^{\alpha'}. \tag{A.10}$$

We also use $\psi$ for the natural homomorphism associated with this relation. Then, the points in the toric diagram are related with the unit vectors in the $\varphi_{\alpha'}$ space $e_{\alpha'}$ by

$$v_{\alpha'} = \psi(e_{\alpha'}). \tag{A.11}$$

By this relation, we can relate the symmetry in the GLSM and that of the moduli space $\mathcal{M}$. The symmetry $\mathrm{U}(1)[e_{\alpha'}]$ acting on $\mathcal{M}_{\mathrm{GLSM}}$ induces the isometry $\mathrm{U}(1)[v_{\alpha'}]$ of the moduli space.

We will now prove the theorem 2:

- In the subspace $\mathcal{M}' \subset \mathcal{M}$ a divisor $F_\alpha$ is given by $\rho_\alpha = 0$.

The restriction to $\mathcal{M}'$ means that we neglect the subspace corresponding to the legs and the center of the web-diagram as we mention in section 5.

It is obvious that if $\rho_\alpha = 0$ the corresponding points in the moduli space is in the divisor $F_\alpha$ because $\rho_\alpha = 0$ is a fixed point of the symmetry $\mathrm{U}(1)[e_\alpha]$, which induce $\mathrm{U}(1)[v_\alpha]$ in the moduli space. What is slightly non-trivial is the converse of this statement. Namely, we need to show that

- If $\psi(\rho)$ is a point inside a divisor $F_\alpha$, then $\rho_\alpha = 0$.

We assume that $\psi(\rho) \in \mathcal{M}'$, and $\psi(\rho)$ is not shared by more than one facets.

Let us choose one corner $\alpha_0$ in the toric diagram, and assume that $\psi(\rho)$ is a point inside a divisor $F_{\alpha_0}$. This means that $\rho$ is invariant under $\mathrm{U}(1)[e_{\alpha_0}]$ up to gauge transformation.

$$e^{i\theta\delta_{\alpha_0}^{\beta'}}\rho_{\beta'} = e^{i\theta\sum_k c_k g_k^{\beta'}}\rho_{\beta'}, \quad (\forall\theta, \beta',\ \exists c_k). \tag{A.12}$$

One trivial solution is

$$\rho_{\alpha_0} = c_i = 0. \tag{A.13}$$

We want to show that this is only solution to (A.12).

Let us assume $\rho_{\alpha_0} \neq 0$. The relation (A.12) with $\beta' = \alpha_0$ requires

$$\sum_k c_k g_k^{\alpha_0} = 1. \tag{A.14}$$

Because $\sum_{\alpha'} g_k^{\alpha'} = 0$ for all $k$ due to the GLSM U(1) anomaly cancellation condition, there is at least one $\beta' \neq \alpha_0$ with which

$$\sum_k c_k g_k^{\beta'} \neq 0. \tag{A.15}$$

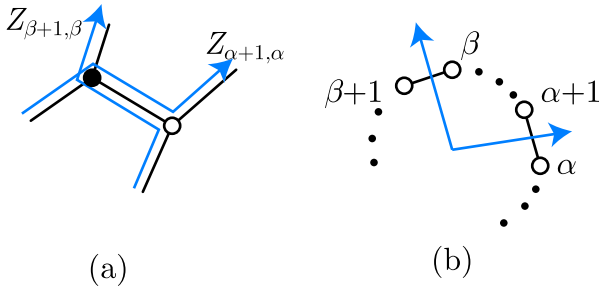


**Figure 19:** (a) shows two zig-zag paths passing through an edge. (b) shows the corresponding external legs in the web-diagram.

If there is only one such a $\beta'$, say $\alpha'_1$, it satisfy

$$\sum_k c_k g_k^{\alpha'_1} = -1. \tag{A.16}$$

From (A.14) and (A.16), we have

$$\delta_{\alpha_0}^{\beta'} - \delta_{\alpha'_1}^{\beta'} = \sum_k c_k g_k^{\beta'}, \quad (\forall \beta'). \tag{A.17}$$

This relation, however, means that $\psi(e_{\alpha_0}) = \psi(e_{\alpha'_1})$, and the two GLSM fields $\rho_{\alpha_0}$ and $\rho_{\alpha'_1}$, and thus two perfect matchings $m_{\alpha_0}$ and $m_{\alpha'_1}$, correspond to the same point at a corner in the toric diagram. This contradicts our assumption.

If there are more than one $\beta'$, say $\alpha'_1$, $\alpha'_2, \ldots$, satisfying (A.15), then from (A.12), we have

$$\rho_{\alpha'_1} = \rho_{\alpha'_2} = \cdots = 0. \tag{A.18}$$

This means that $\psi(\rho)$ shared by more than one divisors and again contradicts our assumption that $\psi(\rho)$ is a point inside the divisor $F_{\alpha_0}$. Therefore, (A.13) is the only solution to the relation (A.12).

### A.3 Theorem 1

Let us prove the theorem 1.

The statement that the set of facets form one continuous region can be shown by using the fact that edge $I$ is always included in two and only two non-parallel zig-zag paths. This means that $m_{\alpha+1}[I] - m_\alpha[I]$ becomes non-zero for two $\alpha$, and they give the boundaries which divide the plane of web-diagram into two parts.

Let $m_{\alpha+1} - m_\alpha$ and $m_{\beta+1} - m_\beta$ be the two zig-zag paths which give the boundaries. There are two possibilities

- case (i) : $m_{\alpha+1}, m_\beta \ni I$, $m_\alpha, m_{\beta+1} \notin I$.
- case (ii) : $m_{\alpha+1}, m_\beta \notin I$, $m_\alpha, m_{\beta+1} \ni I$.



JHEP03(2008)058

In the case (i), because $m_{\alpha+1}$ includes $I$, $Z_{\alpha+1,\alpha} = m_{\alpha+1} - m_\alpha$ passes the edge $I$ from black to white, while $Z_{\beta+1,\beta}$ passes in the opposite direction, from white to black. By the definition of zig-zag paths, we see that $Z_{\beta+1,\beta}$ crosses $Z_{\alpha+1,\alpha}$ upward when $Z_{\alpha+1,\alpha}$ goes left to right. (Figure 19 (a))

This implies that the facets $F_\beta$ and $F_{\alpha+1}$ are on the side of the minor angle made by two legs (figure 19 (b)), and the all facets whose perfect matchings include the edge $I$ are also on the same side. The same is shown for the case (ii) and the proposition has been proved.

## References


[1] A. Hanany and K.D. Kennaway, *Dimer models and toric diagrams*, hep-th/0503149.

[2] S. Franco, A. Hanany, K.D. Kennaway, D. Vegh and B. Wecht, *Brane dimers and quiver gauge theories*, *JHEP* **01** (2006) 096 [hep-th/0504110].

[3] S. Franco et al., *Gauge theories from toric geometry and brane tilings*, *JHEP* **01** (2006) 128 [hep-th/0505211].

[4] B. Feng, Y.-H. He, K.D. Kennaway and C. Vafa, *Dimer models from mirror symmetry and quivering amoebae*, hep-th/0511287.

[5] Y. Imamura, *Anomaly cancellations in brane tilings*, hep-th/0605097.

[6] Y. Imamura, *Global symmetries and 't Hooft anomalies in brane tilings*, *JHEP* **12** (2006) 041 [hep-th/0609163].

[7] Y. Imamura, H. Isono, K. Kimura and M. Yamazaki, *Exactly marginal deformations of quiver gauge theories as seen from brane tilings*, *Prog. Theor. Phys.* **117** (2007) 923 [hep-th/0702049].

[8] A. Butti, *Deformations of toric singularities and fractional branes*, *JHEP* **10** (2006) 080 [hep-th/0603253].

[9] S. Franco and A.M. . Uranga, *Dynamical SUSY breaking at meta-stable minima from D-branes at obstructed geometries*, *JHEP* **06** (2006) 031 [hep-th/0604136].

[10] S. Franco et al., *Dimers and orientifolds*, *JHEP* **09** (2007) 075 [arXiv:0707.0298].

[11] N.J. Evans, C.V. Johnson and A.D. Shapere, *Orientifolds, branes and duality of* $4D$ *gauge theories*, *Nucl. Phys.* **B 505** (1997) 251 [hep-th/9703210].

[12] A. Hanany and B. Kol, *On orientifolds, discrete torsion, branes and M-theory*, *JHEP* **06** (2000) 013 [hep-th/0003025].

[13] Y. Hyakutake, Y. Imamura and S. Sugimoto, *Orientifold planes, type-I Wilson lines and non-BPS D-branes*, *JHEP* **08** (2000) 043 [hep-th/0007012].

[14] O. Bergman, E.G. Gimon and S. Sugimoto, *Orientifolds, RR torsion and k-theory*, *JHEP* **05** (2001) 047 [hep-th/0103183].

[15] H.-C. Cheng and I. Low, *TeV symmetry and the little hierarchy problem*, *JHEP* **09** (2003) 051 [hep-ph/0308199]; *Little hierarchy, little higgses and a little symmetry*, *JHEP* **08** (2004) 061 [hep-ph/0405243].

[16] E. Witten, *An* SU(2) *anomaly*, *Phys. Lett.* **B 117** (1982) 324.


JHEP03(2008)058

[17] A. Hanany and D. Vegh, *Quivers, tilings, branes and rhombi*, *JHEP* **10** (2007) 029 [hep-th/0511063].

[18] D. Martelli, J. Sparks and S.-T. Yau, *The geometric dual of a-maximisation for toric Sasaki-Einstein manifolds*, *Commun. Math. Phys.* **268** (2006) 39 [hep-th/0503183].

[19] R. Kenyon, A. Okounkov and S. Sheffield, *Dimers and amoebae*, math-ph/0311005.

[20] S. Franco and D. Vegh, *Moduli spaces of gauge theories from dimer models: proof of the correspondence*, *JHEP* **11** (2006) 054 [hep-th/0601063].

[21] E. Witten, *Toroidal compactification without vector structure*, *JHEP* **02** (1998) 006 [hep-th/9712028].

[22] I. Affleck, M. Dine and N. Seiberg, *Dynamical supersymmetry breaking in supersymmetric QCD*, *Nucl. Phys.* **B 241** (1984) 493.

[23] I.R. Klebanov and M.J. Strassler, *Supergravity and a confining gauge theory: duality cascades and $\chi$SB-resolution of naked singularities*, *JHEP* **08** (2000) 052 [hep-th/0007191].

[24] S. Elitzur, A. Giveon and D. Kutasov, *Branes and $N = 1$ duality in string theory*, *Phys. Lett.* **B 400** (1997) 269 [hep-th/9702014].

[25] N. Seiberg, *Electric-magnetic duality in supersymmetric non-abelian gauge theories*, *Nucl. Phys.* **B 435** (1995) 129 [hep-th/9411149].

[26] K. Intriligator, N. Seiberg and D. Shih, *Dynamical SUSY breaking in meta-stable vacua*, *JHEP* **04** (2006) 021 [hep-th/0602239].

[27] I. Garcia-Etxebarria, F. Saad and A.M. Uranga, *Supersymmetry breaking metastable vacua in runaway quiver gauge theories*, *JHEP* **05** (2007) 047 [arXiv:0704.0166].

[28] K. Ueda and M. Yamazaki, *A note on brane tilings and McKay quivers*, math.AG/0605780.

[29] K. Ueda and M. Yamazaki, *Brane tilings for parallelograms with application to homological mirror symmetry*, math.AG/0606548.

[30] K. Ueda and M. Yamazaki, *Homological mirror symmetry for toric orbifolds of toric del Pezzo surfaces*, math.AG/0703267.

[31] D.-E. Diaconescu, A. Garcia-Raboso, R.L. Karp and K. Sinha, *D-brane superpotentials in Calabi-Yau orientifolds (projection)*, hep-th/0606180.

JHEP03(2008)058